Degradation of soft subgrade soil from slow, large, cyclic heavy haul road loads: a review

Krechowiecki-Shaw, Christopher; Jefferson, Ian; Royal, Alexander; Ghataora, Gurmel; Alobaidi, Imad

DOI:
10.1139/cgj-2015-0234

Degradation of soft subgrade soil from slow, large, cyclic heavy haul road loads: a review

C. J. Krechowiecki-Shaw, I. Jefferson, A. Royal, G. S. Ghataora, I. M. Alobaidi

C. J. Krechowiecki-Shaw. University of Birmingham School of Civil Engineering, Edgbaston, Birmingham, B15 2TT. CJS518@bham.ac.uk

Prof. I. Jefferson. University of Birmingham School of Civil Engineering, Edgbaston, Birmingham, B15 2TT. I.Jefferson@bham.ac.uk

Dr. A. C. Royal. University of Birmingham School of Civil Engineering, Edgbaston, Birmingham, B15 2TT. A.C.Royal@bham.ac.uk

Dr. G. S. Ghataora. University of Birmingham School of Civil Engineering, Edgbaston, Birmingham, B15 2TT. G.S.Ghataora@bham.ac.uk

Dr. I. M. Alobaidi. Atkins Ground Engineering, The Axis, Birmingham, B1 1TF. Imad.Alobaidi@atkinsglobal.com

Abstract

Extraction of resources in remote locations can require temporary haul roads to transport extremely large, slow-moving, indivisible loads (e.g. plant, oil/gas production modules, reactors, weighing in excess of 1000 tonnes) without interruptions. Poor subgrade soils may experience larger cyclic strains and greater cyclic degradation under these conditions than under conventional roads, yet the short engineering life precludes many foundation strengthening options due to cost. As there is little research into this unique situation, this paper synthesises research from a broad range of applications to discuss implications on expected soil response. Reference is made to critical state theory and Discrete Element Method (DEM) modelling to develop fundamental concepts considering particle-scale interactions. Cyclic failure is proposed to be a kinematically unstable process, triggered by shear banding on the Hvorslev Surface, tensile liquefaction or fabric-governed meta-stable liquefaction; the latter is particularly influenced by stress history and anisotropy. This paper finds pore water pressure accumulation under load and dissipation between loads are key to cyclic degradation and furthermore to be dependent upon load duration, principal stress rotation and repetition frequency. For meta-stable, liquefiable soils in particular, inclination of principal stresses is at least as important in assessing failure risk as magnitude of stresses.

Keywords: cyclic loading, temporary roads, loading rate effects, subgrade soil

1.0 Introduction

Engineering projects, particularly in mineral, oil or gas extraction and power generation, can require very large, indivisible loads (e.g. oil/gas production modules, reactors or large plant) to be transported to remote locations. For example, a conventional trailer may carry 36 metric tonnes per axle, while for exceptional loads a platform composed of multiple Self-Propelled Modular Transporters (SPMTs, Figure 1) can carry 40 metric tonnes per axle (Mammoet 2015a) and cover an area of 3 m to 6 m wide by 10 m to 60 m long (Mammoet 2015b). In the case of the 6 m x 60 m platform, the load (which may be 1000 to 3000 tonnes) will be transferred to the road surface by around 80 relatively closely spaced axles, which will stress a significantly greater volume of soil than conventional traffic. These vehicles typically travel at low speeds, i.e. approximately 5 km/hr, and may recur in the order of once per day.

Heavy haul roads differ significantly from conventional pavement engineering, where the foundation resists a large number of small loads, each inducing a predominantly elastic soil response (Brown, 1996) and cumulative strains affecting the integrity of the bound pavement are the key long-term concern (Frost et al., 2004). Unbound temporary roads designed for construction traffic (e.g. Little 1993; Frost 2000), have greater similarity in that degradation is the primary concern, however differences in scale mean direct comparisons cannot be drawn. Furthermore, heavy haul roads permit greater strains and have a much shorter design life, but mobilise a significant proportion of the soil's bearing capacity, particularly in soft normally consolidated deposits below the water table (which may be too deep to receive stresses from smaller vehicles). Clearly the risk of cyclic degradation and deep bearing failure are greatly increased.

Unlike a motorway or railway, which represents a long-term economic and social investment, a temporary haul road is by definition a short-term venture, facilitating the transportation of equipment to site. Sufficient robustness to avoid subgrade failure and damage to equipment and/or production delays is required, but at minimal cost. Running repairs to the road may be acceptable, depending on logistical implications (delays, material supply, etc.)

This paper aims to describe potential mechanisms for cyclic degradation and failure of a soft saturated subgrade, ultimately likely to be a function of pore water pressure accumulation. Factors unique to the heavy haul road problem, i.e. slow loading rates and infrequent repetitions, are examined: slower cyclic loading rates accumulate greater pore pressures, drainage between loads allows dissipation and strengthening. Cyclic failure modes are identified as kinematically unstable, rapidly accumulating large strains if a threshold stress level is exceeded.

This situation presents challenges to the designer with numerous uncertainties in the subgrade soil behaviour. Cost pressures and uncertainties in applying analytical design to the field (e.g. soil heterogeneity, limitations of ground investigation), call for an observational design approach to be embraced, i.e. using monitoring to support a leaner design and inform repairs. Commentary on suitable *in-situ* monitoring is provided within to help facilitate such a design approach. Literature from other geotechnical disciplines with similar cyclic loading concerns has been reviewed, including shallow foundations (both onshore and offshore) and earthquake engineering alongside conventional road and railway foundations, focusing on the following aspects in the context of heavy haul roads:

- Distribution and form of subgrade stresses in an unbound road
- Cyclic failure and the threshold stress concept
- Static and cyclic liquefaction
- Changes to soil behaviour from cyclic loading
- Timescale implications; drainage of residual pore water pressures and loading rate effects.

The following symbols are used in the paper:

q: deviator stress (kPa)

p’: mean effective normal stress (kPa)

e: void ratio (-)

p'_e: equivalent mean effective normal stress on normal compression line (kPa)

2.0 Distribution and Form of Subgrade Stresses

2.1: Stress transfer and response of unbound roads

Unbound granular roads have been studied extensively in terms of; their ability to distribute wheel loads, the recoverable (or resilient) deflection under transient loads and accumulation of permanent strain causing rutting (e.g. Hyde 1974; Little 1993; Wolff and Visser 1994; Frost 2000; Ravi et al. 2014). Studies by Little (1993) and Frost (2000) are of particular relevance to the heavy haul road problem as they address the in-situ behaviour of unbound roads carrying low volumes of heavy traffic.

Failure of unbound roads is progressive in nature; permanent strains accumulate over time, leading to rut development (Little 1993; Wolff and Visser 1994; Frost 2000). For a temporary heavy haul road, the development of ruts constituting serviceability failure of a permanent unbound road, (e.g. 10-20mm; Wolff and Visser 1994) may be acceptable if further development is slow. Rapid initial rutting followed by stabilisation, likely to be due to compaction of the granular layers, was observed on trial road sections by Little (1993) and Frost (2000) and can be controlled by running repairs. However avoidance of runaway deflections controlled by subgrade degradation which does not stabilise, as observed by Little (1993), should be the focus of the design of heavy haul roads.

The progressive failure mechanism depends upon the response of granular layers, subgrade soil and the interaction between them. Depending upon the density, grading, confining stress of granular materials and the transient load applied, strain may accumulate initially before stabilising (shakedown) or may reach a state where strain continuously accumulates, known as ‘ratchetting’ (Werkmeister et al. 2004; Pérez and Gallego 2010). Brown and Chan (1996) observed the onset of such progressive failure in granular materials to occur sooner in more poorly graded materials and under higher wheel loads, and Frost (2000) observed that when poorer capping materials were used, development of rapid rutting occurred which was predominantly confined to the road layers. A similar progressive failure also occurs in clay subgrades (discussed in depth in Section 3).

The concept of shakedown and progressive plastic failure can be applied to the interaction between the road and subgrade. Various authors have modelled road structures as layers of elastic-perfectly plastic material (Sharp and Booker 1984; Boulibane et al. 2005; Zhao et al. 2008) and found initial plasticity followed by shakedown is possible for loads initially causing local yield if a residual stresses field can develop to counteract yielding (in both the pavement and subgrade). Sharp and Booker (1984) found stiffer pavement layers increases the failure load for the subgrade but reduces the failure load for the pavement; increasing pavement stiffness beyond an optimal value can decrease its capacity. Increasing pavement depth (whilst maintaining other properties constant) was found to increase the failure load in the subgrade; deeper pavements spread the subgrade load further without concentrating stress in the pavement layer. Shakedown analysis of unbound roads by Boulibane et al. (2005) similarly found the pavement strength limited the ultimate capacity above a certain thickness. This limit increased significantly with the angle of shearing resistance of the pavement (corroborated by cohesive-frictional shakedown analysis by Zhao et al., 2008, which found the result to be highly sensitive to the angle of shearing resistance), but was influenced little by its cohesion. These analyses indicate the load-spreading properties of the pavement layers, dictated by the material quality, to be critical to governing whether shakedown or progressive failure occurs. Sufficient stiffness to spread load and sufficient strength to avoid failure within the pavement are required to control subgrade plasticity. Whilst useful in understanding the response of the composite system, a fundamental shortcoming of these shakedown analyses is that material parameters are assumed to be constant throughout, which may be reasonable when small strains are applied to a subgrade. However, as is discussed in this paper, soil response changes as a result of induced pore water pressures, time-dependence and induced volume strains, particularly when cyclic subgrade strains are large.

To relate fundamental phenomena to field response, understanding how stress is transferred to the subgrade under heavy traffic is vital. Unbound granular pavements exhibit non-linear stiffness which depends upon the strain and mean effective normal stress (Wolff and Visser 1994; Brown 1996) and so changes during passage of a load. When stresses remain within the yield strength, a non-linear elastic model for unbound road materials is considered sufficient (Wolff and Visser 1994). Measurement of subgrade stress from passage of 80kN and 126kN axles over an unbound road by Little (1993) found good agreement with non-linear elastic models but a linear elastic model overestimated subgrade stresses for the larger load by more than 30%.

The magnitude of the soil zone stressed by load applied to an unbound road is also important. Field dynamic stiffness tests on the subgrade and the top of capping by Frost (2000) found that for the larger capping thickness (over 300 mm), the capping rather than the subgrade tended to dominate the results. Interestingly a thin layer of stiffer sub-base over the smaller capping thickness (less than 300 mm) had little effect on the composite stiffness, as the layer was too thin relative to the stressed zone which was dominated by the softer subgrade. The influence of a stiffer, unsaturated upper subgrade layer on unbound roads is also noted by Little (1993), who found pavements designed to reach a failure mechanism performed adequately as a result of exceptionally dry weather producing a stiff crust. A larger stress bulb would be influenced to a lesser degree by the upper layers of significantly stiffer granular material and unsaturated or overconsolidated subgrade, similar to the thin layer effect observed by Frost (2000).

Results of a simple plane-strain analysis based on the parameters in Table 1, incorporating a non-linear elastic model for the unbound road and linear elastic subgrade soil, are provided in Figure 2. The unbound road is modelled as a modified Mohr-Coulomb material which is similar to the K-Theta model used by Little (1993) and Wolff and Visser (1994); the stiffness has a power-law relationship (Table 1) with the mean effective normal stress, and cohesion is set sufficiently high that no yield occurs. The effects of local yielding and stress redistribution are not considered in this elastic model, hence it can only be considered a crude approximation of the stress field under a heavy haul vehicle. Nevertheless, it provides an approximation of the interaction between the various wheel loads. Elastic models represent the lowest degree of lateral load-spreading. Localised yielding and redistribution under increasing shear will tend to make stress spread laterally more readily, meaning greater interaction, as the ultimate bearing capacity is approached and strains become increasingly localised to the slip surface (Osman and Boulton 2005).

Stress contours in Figure 2 indicate heavy haul road vehicles with a similar wheel layout to the SMPTs in Mammoet (2015a) have stress bulbs from the wheel loads which join together to create a stress bulb on the scale of the vehicle. This is similar to the finite element model results by Gräbe and Clayton (2009) which found combination of individual sleeper loads at depth beneath a railway. Therefore, unlike most of the studies on unbound roads to date, global progressive failure of a heavy haul road can be characterised as an extremely thin pavement layer relative to the load and as such will be dominated by the subgrade's response to cyclic load rather than load-spreading of the pavement. Furthermore, it will be the soil at depth, which may be saturated and closer to a normally consolidated state, which will govern the failure mechanism. Bearing in mind the expected dominance of deeper strata, ground investigation for these projects will need to focus on investigation and monitoring at depth (similar to a large shallow foundation) rather than the surface tests typically used.

Loading of deeper, saturated and normally consolidated soil also means the assumption of strain being largely recoverable may no longer hold. Finite element settlement predictions using linear elastic, perfectly plastic models (D'Appolina et al. 1971) diverge from elastic predictions in normally consolidated soil at below 20 % of ultimate bearing capacity, indicating plastic stress redistribution. In lightly overconsolidated soil (which is more likely to be the governing subgrade stratum beneath a conventional road) yield may not occur below 40 % to 60 % of ultimate capacity (D'Appolina et al. 1971). Large strains and plastic stress redistribution is likely under heavy haul roads, where loads may mobilise similar proportions of capacity to conventional shallow foundations, i.e. 33 % to 50 % (BSI, 1986) or even higher.

2.2: Principal stress rotation

Moving wheel loads also result in rotation of principal stresses (Brown, 1996). This causes plastic strain without requiring an increase in deviator stress, reduces stiffness and causes a more ductile response (Arthur et al. 1980; Zdravković and Jardine 2001). However changes to strength with principal stress rotation were observed to be less marked. Pore water pressures also accumulate at increased rates (Gräbe and Clayton 2009; Xiao et al. 2014) for the same deviator stress when principal stress rotation is included. Greater volume contraction from inclined consolidation (Zdravković and Jardine 2001) means settlements of haul roads will be difficult to predict and have limited use for planning maintenance interventions based on observation; monitoring pore pressures at depth may be more effective in indicating risk levels. Understanding stress rotation is particularly important in meta-stable, liquefiable deposits: undrained strength of sand reduces significantly as major principal stress increasingly aligns with bedding planes (Sivathayalan and Vaid 2002). Heavy haul roads over liquefiable soils in particular will need to limit stress rotation as well as the magnitude of deviator stress to safeguard against failure.

Failure mechanisms vary depending on principal stress reversal; Selig and Chang (1981) and Andersen (2009) found that triaxial tests subject to roughly equal maximum compression and extension stresses showed little accumulation of permanent strain but instead produced large transient strains at failure. Conversely, tests where only small extension stresses (or no stress reversal) were applied accumulated permanent strain at increasing rates, with a lesser tendency to develop increased transient strains. Degradation in soil loaded in extension by heavy haul vehicles may therefore exhibit minimal strain as a result of ongoing degradation, unlike the compression zone. It may therefore be difficult to monitor risk through surface movement. Again, pore water pressure measurement will be much more effective in characterising degradation.

Unlike a conventional road pavement, overburden stresses on the deep failure mechanism will not be negligible in comparison to transient stresses (Brown, 1996). Therefore, soil at depth below the vehicle centreline may not experience large principal stress rotation but simply cyclic variation of compressive stress

(Figure 3), whereas soil at shallow depth and away from the vehicle centreline may experience complete principal stress reversal. The development of progressive failure will depend upon both the relative rates of degradation in these different zones, and the ability of the soil to drain these excess pore water pressures and strengthen (discussed later herein).

3.0 Cyclic Failure and Threshold Stress

Cyclic degradation of a clay subgrade is progressive (similar to the granular materials discussed previously), with strain and excess pore water pressure developing over time. Defining the exact point of a progressive cyclic failure is difficult; much of the literature uses definitions based on a failure strain, e.g.: ± 3 % cyclic strain (Brown et al., 1977); 15 % average or cyclic strain (Andersen et al. 1988) and 1 % permanent strain (Frost et al. 2004). Such disparity may appear an obstacle to clearly defining failure. However as cyclically loaded soil develops most strain in the last few cycles before failure (Overy 1982; Ward 1983; Li et al. 2011), numbers of cycles to failure is not significantly affected by the defined failure strain, within sensible limits (e.g. those stated above). Conversely, increasing tolerance of subgrade strain for heavy haul roads may not significantly lengthen design life. In fact, large shear displacements of the order of 100 mm to 300 mm may result in shear strengths being reduced to low residual values in clays (Skempton 1985) making subsequent remediation much more costly, as Skempton (1995) exemplified in the case of early railway earthworks.

Heath et al. (1972) found a divergent strain response related to a threshold stress: strains stabilised for cyclic stress below the threshold and accelerated for cyclic stresses above (Figure 4). Threshold stress has commonly been normalised to a soil's maximum static deviator stress. Factors controlling this relationship are not clear and significant variation is observed, suggesting further research into this phenomenon is required. Ward (1983) for example summarises a number of studies on different soils; normalised threshold stresses vary between 37 % and 96 % with no clear trends apparent. Experiments on natural clays by Frost et al. (2004) show large scatter, with normalised threshold stresses falling within 25 % to 100 %. Threshold stress for a given soil also varies depending on overconsolidation (Ward 1983) and the ratio of static to cyclic shear stress (Andersen et al., 1988). Frost et al. (2004) suggest the conservative lower bound on normalised threshold stress of 25 % proposed by Heath et al. (1972) is reasonable; however for temporary roads such conservatism is less desirable.

Nicot and Darve (2010) state bifurcation (in this context, a divergence of strains from similar initial conditions) implies kinematic instability and transition to a dynamic state, accompanied by rapid increase in soil kinetic energy. Thus the rapidly increasing strains approaching cyclic failure imply a kinematically unstable process. The highly successful Cam-Clay model of Schofield and Wroth (1968) states wet-of-critical soils loaded to the critical state are kinematically stable and ductile. Kinematically unstable failure modes, i.e. shear banding on the Hvorslev Surface, tensile liquefaction occurring on the dry side of critical and static liquefaction on the wet side of critical, are therefore considered below in the context of cyclic failure.

4.0 Undrained Cyclic Failure in the Critical State Model

Undrained cyclic loading in a wet-of-critical state causes accumulation of positive pore water pressures in a range of soils including clays, sands and sand-silt-clay composites (Overy 1982; Marto 1998; Gratchev et al. 2006; Li et al. 2011; Åhnberg and Larsson 2012). Schofield and Wroth (1968) suggest rising pore water pressure indicates load shedding from soil skeleton to pore fluid. The soil skeleton must still resist the deviator stress (pore fluid has no shear strength) so confining stress is lost. Andersen (2009) suggests lost particle contacts under cyclic load, manifested as increased pore water pressure, causes strength loss. Discrete Element Method (DEM) simulations of force distribution in granular assemblies indicate a series of 'strong' networks (i.e. carrying greater than average contact forces) principally supports deviator stress (Gong, 2008) 'Weak' networks, carrying low contact forces, orthogonally restrain these 'strong' networks. If 'weak' restraint is lost, rearrangement and large straining can occur in a buckling-like manner (Nicot and Darve 2010). Soroush and Ferdowsi (2011) found DEM contact forces become more anisotropic with each cycle of strain-controlled loading (Figure 5) and Thornton (2000) states DEM-simulated shear deformation causes separation of particle contacts orthogonal to the deviator stress. A similarly increasing anisotropy is found with simulation of stress-controlled cyclic loading by Xu et al. (2015). These findings support the hypothesis that cyclic degradation is the result of contact breakage, reducing 'strong' network confinement. DEM simulations use frictional contact laws (Gong, 2008), thus these findings are not necessarily applicable to clays, which also have electrostatic particle interactions (Keedwell 1984). However DEM simulation by Anandarajah (2000), which modelled clay platelets as thin, slender particles with electrostatic face and edge forces, found the stress-strain response was controlled by cluster-to-cluster (rather than platelet-to-platelet) forces. Relative importance of electrostatic forces on macro-behaviour is therefore reduced.

Soil reaching the Hvorslev Surface can fail locally in a brittle manner along a shear band (Schofield & Wroth, 1968); the likelihood of such a failure is increased by non-uniformity (Atkinson 2007). Nova (2010) demonstrated that internal stress transfer along a shear band, resulting in kinematic instability, can be caused by local stress or strain non-uniformity; a heterogeneous soil is clearly at greater risk of cyclic degradation. Cyclic tests conducted by Ward (1983) on normally consolidated and lightly overconsolidated silty clay indicate failure when effective stress paths intercept the Hvorslev Surface (Figure 6), with shear bands typically observed. This failure mode is not universal: dry-of-critical static tests can fail at the critical state (Hyde 1974; Brown et al. 1975). Brown et al. (1975) also observed dry-of-critical cyclic tests to accumulate negative excess pore water pressures at increasing rates under cyclic load. Ward (1983) suggested observed cyclic failure on the Hvorslev Surface was due to non-uniformities inherent from preparation of the small (37 mm diameter) samples used. It is worth noting that natural soils, particularly soft alluvium which may contain a mixture of sand, silt and clay, are rarely uniform in composition. Monitoring excess pore water pressures in saturated subgrades, in comparison to those required to reach the Hvorslev Surface, should therefore provide a useful indication of the proximity to failure. Trigger levels for intervention can be set on this basis.

5.0 Liquefaction from Undrained Cyclic Loading

5.1: Mechanisms for Liquefaction

Muhunthan and Worthen (2011) proposed that stable soils only liquefy upon reaching the tension cut-off; a hydraulic gradient accelerates cracking, causing kinematically unstable fluidization. This definition purposefully omits liquefaction for contractive soils, as observed by Been and Jeffries (1985) in undrained loose sands, deeming this to be inherent metastability (Muhunthan and Worthen 2011). Unlike tensile liquefaction, which requires large cumulative pore water pressures (Figure 6), metastable liquefaction occurs with smaller excess pore water pressures at low strains (Lade 1994). In-service detection capabilities are therefore limited; heavy haul road design must instead aim to identify and mitigate at-risk areas prior to loading.

Static liquefaction occurs when contractive, undrained soil reaches a peak deviator stress at a consistent mobilised angle of shearing resistance (Been and Jeffries 1985). Liquefaction occurs regardless of whether the stress is entirely undrained or as a result of a small undrained increment to a drained stress (Lade, 1994). Static stresses from haul road earthworks increase the friction angle mobilised in the drained condition. This may therefore increase, rather than decrease, the risk of static liquefaction from undrained stress increments from traffic. Whilst recovery can occur (Lade 1994; Yamamuro and Lade 1999), strains are so large that static liquefaction can be treated as failure (Figure 7). Liquefaction is impossible if excess pore water pressures can dissipate (Lade 1994) so is unlikely where heavy haul roads cross loose, clean sands. Silty or clayey sands may be sufficiently impermeable to be at risk of static liquefaction.

5.2: Influence of Coarse-Grained Soil Fabric

Lade (1994) proposed the small strain required to initiate static liquefaction indicates the phenomenon is governed by soil fabric. This fabric-dependence was investigated further; when non-plastic fines were added to sand, peak deviator stress reduced, hypothesised to be due to fines forming an open microstructure (Yamamuro and Lade, 1999). Similarly undrained cyclic tests by Gratchev et al. (2006) found small quantities of low plasticity fines reduced liquefaction resistance. Microscopic imaging confirmed that fines formed weak connectors between sand grains; as the Plasticity Index of the composite soil rose above 5 % to 14 %, soils became more resistant to liquefaction with fines forming a stabilising matrix (Gratchev et al, 2006). Liquefaction resistance also increased when angular crushed glass fines were mixed with uniform sand instead of smooth glass spheres (Wei and Yang 2014), further supporting the hypothesis of Yamamuro and Lade (1999).

Fabric-dependent resistance to liquefaction can be simulated by DEM. Nouguier-Lehon (2010) was able to show that hexagonal particles developed additional rotation resistance when compared to circular particles, partly due to their ability to make face-to-face contacts. The texture of particles is also important: in three dimensions, a completely frictionless sphere will require six reaction points to maintain static equilibrium, which reduces to four for infinitely frictional particles(Thornton 2000). Increasing particle friction also causes greater dilation under shear (Kruyt and Rothenburg 2006). DEM simulations by Gong (2008) found the coordination number (average number of contacts per particle) reduced during undrained shear and the onset of liquefaction occurred at a statically determinate state (Figure 8). The observed phase transformation and static liquefaction were considered equivalent to forming a mechanism. As frictional, elongated and angular particles are able to remain static with fewer contacts, more contacts must be broken to liquefy. Well-graded materials have increased resistance, due to more contacts being initially available.

Fabric may be rearranged by loading, which implies more optimal arrangement to resist the previously applied load (Been and Jeffries 1985) and may cause weakening in another direction. This is found in DEM; deviator stress orientates normal contact forces increasingly anisotropically (Gong, 2008; Zhao and Evans, 2011) and anisotropy of the assembly's elastic stiffness matrix develops (Kruyt 2010). Anisotropy of liquefaction resistance is also apparent: Doanh et al. (2012) showed a cycle of drained compressive deviator stress (in a triaxial cell) applied to contractive sand increases peak stress in subsequent undrained compression, but reduces peak stress in extension (Figure 9). When preparing liquefiable subgrades to carry a heavy haul road, applying and removing compressive surcharge to soil which is subsequently taken into extension by transient loads may increase rather than reduce liquefaction risk. Compaction using large rollers for example, which rotates principal stresses, or placing a permanent surcharge in the form of a berm to avoid extension under transient loads, may be more effective.

5.3: Meta-Stable Liquefaction in Fine Soils

Meta-stable liquefaction does not solely apply to coarse-grained soils. Sensitive clays have a highly open microstructure and their shear strength is lost upon remoulding, resulting in liquefaction (Åhnberg and Larsson 2012). Experiments indicate various clays exhibit limited meta-stable liquefaction with peak deviator stress reached wet-of-critical before the critical state, for example in London Clay and Kaolin (in Schofield and Wroth 1968), Bothkennar clay (Allman and Atkinson 1992) and marine clay (Li et al. 2011). Cyclic tests on Keuper Marl (now known as Mercia Mudstone) by Overy (1982) rapidly gained pore water pressure on the wet side of critical, particularly at high stress, suggesting meta-stable liquefaction; in this case, possibly due to Mercia Mudstone's clay fraction forming aggregations prone to breakage under cyclic load (Chandler and Forster 2001). Meta-stability may therefore be influential in cyclic response for a wide range of soils and the authors recommend further research into this influence.

6.0 Changes in Deformation and Pore Water Pressure Response with Cyclic Loading

Cyclic loading induces changes to the stress state and fabric of the soil, which can fundamentally alter the soil's response to subsequent load. Contractant soil can become dilatant and normally consolidated soil previously showing strain-hardening behaviour can exhibit strain-softening failure. The latter is of greater concern to the stability of heavy haul roads; these issues are explored in greater detail below.

6.1: Pore Water Pressure, Stress Path and Resilient Strain Response

Normally consolidated soils not reaching cyclic failure accumulate positive pore water pressures at decreasing rate, often stabilising to near-zero rates at large numbers of cycles (Hyde, 1974; Ward 1983;

Marto 1998, Figure 10). Hyde (1974) and Ward (1983) observed similar accumulation of permanent strain under one-way cyclic loading and integrated these rate relationships to predict strains and pore water pressures respectively with some success. However the assumption of linear rates after large numbers of cycles appears to provide generally conservative estimates.

Static strength of normally consolidated soil has been observed to reduce following large cyclically-induced strains and pore water pressures, (e.g. Brown et al. 1977; Togrol and Güler 1984; Andersen et al., 1988; Li et al. 2011). Ward (1983) found samples accumulating sufficient pore water pressure failed on the Hvorslev surface under subsequent static load, at lower deviator stress than the critical state. Induced overconsolidation was considered to be the primary mechanism for strength loss in such cases. Togrol and Güler (1984) and Li et al. (2011) similarly explained their observed reduction in strength following cyclic loading as a function of induced overconsolidation. Ward (1983) found normalised pore water pressure behaviour at failure (quantified by Skempton's pore water pressure parameter, A) was similar between overconsolidated and post-cyclic samples. This was thought to indicate the changes to effective stress paths for normally consolidated samples experiencing cyclically-induced pore water pressures are equivalent to overconsolidation. This is further corroborated by recent work by Wang et al. (2015), in which silt samples liquefied by undrained cyclic loading were observed to follow similar behaviour (when normalised by effective confining pressure) to those overconsolidated to the same state by static swelling.

A fundamentally different explanation is given by Carter et al. (1982) who modelled shrinkage of the wet-of-critical yield surface from cyclic loading (Figure 11, c.f. Figure 6). This model is able to reproduce pore water pressure accumulation, cyclic effective stress paths and post-cyclic loss of strength observed experimentally. However this model implies the soil remains in a wet-of-critical state up to failure on the critical state line and does not consider induced overconsolidation from excess pore water pressures. Furthermore, inherent soil variability makes direct comparison of yield surfaces before and after cycling difficult. A model such as that proposed by Pender (1982) or Li et al. (2011), which describes changes to yield surfaces due to stress state and overconsolidation, may be more effective.

Resilient modulus and effective confining stress in clays reduce to a stable value during cyclic loading below the threshold stress (Brown et al. 1975; Overy 1982; Frost et al. 2004). A relationship between resilient modulus and the ratio of effective confining stress to deviator stress from cyclic tests below the threshold stress for silty clay (Brown et al. 1975) was found to be applicable to a wide range of overconsolidation ratios. This similarly suggests particle contact breakage (particularly orthogonal to load; Figure 5) manifested by rising pore water pressure, is critical in describing soil cyclic response and changes induced are similar to overconsolidation.

In unsaturated soils above the water table, as is often the case for pavement foundations, effective stress and therefore strength is provided primarily by pore suctions (Brown, 1996). There are a number of mechanisms by which unsaturated soil can lose suction. Compaction under load removes air, reducing specific volume so volumetric water content increases, reducing suction (Jaquin et al. 2009; Guan et al. 2010). Contractive soils close to saturation reduce suction under shear (Toll and Ong 2003). Dilating materials with low degrees of saturation can also lose suction under shear if water is held within clay aggregations: clusters are compressed, ejecting water into the macro-pores (Toll 1990; Jaquin et al. 2009). Menisci within macro-pores primarily provide the suctions which resist shear (Toll 1990; Toll and Ong 2003; Jaquin et al. 2009); wetting these pore spaces or shearing menisci can result in rapid loss of strength.

6.2: Fabric Rearrangement and Induced Anisotropy

Strength is not necessarily reduced after cyclic loading. Brown et al. (1977) found static strength of isotropically normally consolidated silty clay samples experiencing maximum cyclic strains less than ± 3 % immediately improved compared to their pre-cyclic static strength. The failure envelope was found to be translated to match overconsolidated samples (same internal angle of shearing resistance, increased effective cohesion).This strength increase cannot be related to changes in stress state (i.e. increased pore water pressures), which implies reduced strength; fabric rearrangement is the most likely cause. Beneficial fabric rearrangement is similarly implied by increasing resilient modulus of saturated soil under low cyclic stress (Ward 1983; Ng and Zhou 2014). Smaller increases in resilient modulus for unsaturated soil with increasing suction (Ng and Zhou 2014) further support this hypothesis: unsaturated soil better maintains its initial fabric through pore suctions (Toll and Ong 2003) so resists beneficial rearrangement.

Under stress-controlled cyclic loading, most strain develops at the end of each half-cycle at maximum and minimum deviator stress (Overy 1982; Åhnberg and Larsson 2012), suggesting most micro-structural rearrangement occurs here. Isihara and Towhata (1982) differentiate between primary plasticity, occurring when the stress path reaches a shrinking yield surface and secondary plasticity, occurring within this yield surface (Figure 12). This implies continual small rearrangements under cyclic load, with greater rearrangement when the stress state becomes more anisotropic than previously encountered.

DEM simulations illustrate that increasing deviator stress results in increased proportions of contacts frictionally sliding, causing plasticity on a macro-scale (Kruyt 2010). Slippage does not occur on heavily loaded ‘strong’ contacts (Soroush and Ferdowsi 2011) but is more likely on ‘weak’ inter-particle contacts. In granular assemblies (where deviator stress is transmitted primarily as normal forces; Thornton 2000), increasing anisotropy of contact forces (through increasingly anisotropic stress) causes ‘strong’ networks to lose restraint and rearrange, resulting in large plastic strains. Based on the above, the authors propose primary plasticity occurs once restraint is lost to ‘strong’ networks, while secondary plasticity is small rearrangements to ‘strong’ networks while restraint remains sufficient. This is exemplified by DEM simulations of cyclic load by Sazzad and Suzuki (2010); in the stiff part of a cycle, anisotropy of the ‘strong’ network changes rapidly. During the softer response, anisotropy of the ‘strong’ network does not significantly change whilst overall anisotropy increases (Figure 13), suggesting reduction of restraint coincides with softer response. Secondary plasticity, which maintains restraint, may cause beneficial fabric rearrangement under undrained cyclic loading observed experimentally.

7.0 Time-Dependent Behaviour

7.1: Drainage and Consolidation

Drainage of positive excess pore water pressures reduces void ratio, increasing critical state strength; swelling from negative pore water pressure reduces critical state strength (Schofield and Wroth, 1968). Tests by Brown et al. (1977) on Drammen Clay indicate drainage of residual pore water pressures following cyclic load significantly improves strength of normally consolidated clay, slightly improves lightly overconsolidated clay and has either no effect or slightly weakens heavily overconsolidated clay. Scale model tests applying cyclic load to a clay subgrade by Ravi et al. (2014) similarly demonstrated that as the induced pore pressure dissipated, the strength of the subgrade (prepared to be close to a normally consolidated state) increased. A more dilatant response was also apparent, implying induced overconsolidation. Similarly tests by Overy (1982; Figure 14) found samples initially failing under cyclic loading were observed to withstand increased numbers of cycles before failure and eventually stabilise if drainage of residual pore water pressures between loading periods was permitted. This apparent increase in threshold stress (compare Figure 14 to the response in Figure 4) from drainage merits further study, as a fuller understanding may permit more cost-effective temporary infrastructure.

In low permeability soils, partial dissipation of residual pore water pressures can cause failure (similar to Figure 6) if accumulation exceeds drainage, as effective stresses can still reduce to intercept the Hvorslev Surface or tension cut-off. Volume contraction may increase consolidation time: Dewhurst et al. (1996) found under one-dimensional consolidation of low-permeability clay (tested range of 10^{-10} m/s to 10^{-12} m/s), the logarithm of permeability decreased linearly with mean normal effective stress. Reduced compressibility from densification (O'Riordan 1991) conversely often counteracts this effect to accelerate consolidation; the overall effect depends on the relative changes to both. Cyclically-induced volume collapse of a meta-stable soil could reduce permeability without the expected reduction in compressibility. This may cause slower excess pore water pressure dissipation. Consolidation times from one-dimensional analysis are typically overestimated (Davis and Poulos 1972) due to two or three dimensional drainage paths and permeability anisotropy (particularly silt/sand partings). Monitoring pore water pressures can control these uncertainties, avoid unnecessary delays from overestimated consolidation times and reduce subgrade damage by waiting for dissipation before reloading.

Undrained cyclic loading of wet-of-critical soils induces overconsolidation, moving the stress state closer to failure (Figure 6). Subsequent drainage reduces apparent overconsolidation, provided the gradient of volume change against effective stress is less than that on the virgin compression line (Figure 15). Reduction in overconsolidation, as well as increasing strength, was observed by Wang et al. (2015) when liquefied samples were allowed to drain. The volume change gradient is influenced by preceding stress conditions: samples failing cyclically had a much steeper gradient, in some cases parallel with the virgin compression line, while those which remained stable followed a gradient similar to the swell-back line (Overy 1982, Figure 13). This behaviour was similar to that observed by Brown et al. (1977). O'Riordan (1991) shows similar reduction in volume change gradient with successive repetitions of a cyclic oedometer test. Large volume change gradients may imply metastable liquefaction and restructuring similar to Figure 7 and Figure 8 (the samples of Overy, 1982, failed cyclically wet-of-critical at 0.6 % strain). Volume change parallel to the virgin compression line fully retains apparent overconsolidation (Schofield and Wroth, 1968), although the proportion of strength mobilised by a constant cyclic stress reduces with reduction in void ratio (Figure 15). Greater densification means pore water pressures induced by subsequent load are much lower and risk of failure from induced overconsolidation is low. These large drainage-induced volumetric strains may cause large settlements in areas at risk of metastability; subgrade compaction and densification is advisable to avoid costly repairs and delays. On-plant instrumentation, used to monitor compaction (e.g. smart rollers), can be used to further characterise soil behaviour and assist the engineer in identifying and remediating problematic areas.

7.2: Loading Rate Effects and Rheology

Deformation and pore pressure response of fine-grained soils, in particular, has been observed to be a function of the loading rate (Overy 1982; Teachavorasinskun et al. 2002; Li et al, 2011). Therefore to understand the subgrade response for heavy haul roads the loading frequency and strain rates must be selected to best simulate those *in-situ*. For example a 60 m long module travelling at 5 km/hr may apply a load for 45 seconds, equivalent to a period of 0.02 Hz. In contrast, much of the literature uses faster rates than apply to heavy haul roads: Heath et al. (1972) at 0.5 Hz, the majority of Overy (1982) at 0.1 Hz, Andersen et al. (1988) at 0.1 Hz, Frost et al. (2004) at 2 Hz. This generates a different undrained response, as discussed below.

Similar accumulation of pore water pressure and strain of soil under undrained creep to Figure 10 (Singh and Mitchell 1968; O'Reilly et al. 1988) indicates rheology may provide good analogy to cyclic loading at different rates. Hyde (1974) and Li et al. (2011) use creep analogy to predict cyclic deformations of clays below failure with good accuracy at low stresses and strains, but becoming less reliable once strain rate begins to accelerate to failure. Li et al. (2011) unify strain accumulation for sinusoidal cyclic stress at different frequencies by plotting against time, which is accurate until cumulative strain exceeds the static failure strain (around 3 %) and strain rate accelerates to failure.

Overy (1982) indicates shear strength of silty clay increases and lower pore water pressures are generated (the effective stress path rises closer to vertical in normalised q, p' space) at faster strain rates. Teachavorasinskun et al. (2002) observed stiffness of intermediate plasticity clay increased with strain rate, while pore water pressure was largely unaffected, when exposed to small (< 0.2 %) strains. Conversely stiffness varied little, while excess pore water pressures reduced with increasing strain rate, when exposed to larger strains. The concept of time-dependent contact forces (Keedwell 1984) can explain this type of response: time-dependent inter-particle slippage is small, without significant additional loss of contacts (similar to secondary plasticity discussed earlier), over small strains, i.e. close to the cyclic pore pressure threshold strain (Hsu and Vucetic 2006), which may be in the order of 10^{-1} to 10^{-2} % strain in cohesive soils (Díaz-Rodriguez and López-Molina 2008). Over larger strains, i.e. approaching the cyclic degradation threshold in the order of 0.5 % to 3 % strain (Díaz-Rodriguez and López-Molina 2008), time-dependent slippage causes increased contact breakage and loss of restraint (i.e. primary plasticity). DEM shear simulations by Gu et al. (2013) found at similar strains (less than 1 %), the tangential force anisotropy reaches a peak before dropping rapidly (indicating frictional slippage), after which the anisotropy of contact normal planes increases rapidly (indicating particle rearrangement). Above the cyclic degradation threshold strain it is therefore reasonable to expect the soil behaviour to be governed by sliding and rearrangement of inter-particle contacts, which are expected to produce a time-sensitive response, particularly in clays.

Under the large strains and slow rates of load application expected from heavy haul road traffic, primary plasticity will be more apparent than for faster, conventional traffic. Comparison of slow haul road traffic to threshold stress relationships derived from faster load application rates, without consideration of rate effects, can significantly overestimate threshold stress, as noted by Ward (1983). Over the anticipated loading timescales, excess pore water pressure drainage is small in fine-grained soils and will not provide benefit.

Vaid (1988) found similarity between failure strain in strain-controlled triaxial tests (at different strain rates) and the strain at which minimum strain rate occurred in stress-controlled creep tests (corresponding to the point beyond which strain accelerates to failure) in low plasticity clay. Vaid (1988) proposed a unique relationship in stress, strain and strain rate space, further corroborated by multi-stage tests. Identification of similar commonality in cyclic loading would allow predictions over a wide range of conditions from fewer, carefully selected tests.

Cyclic tests by Åhnberg & Larsson (2012) indicate such commonality. Once the accumulated permanent strain reached the static failure strain in stress-controlled cyclic loading, deformation began to accumulate at increasing rate rather than a decreasing rate (similar to Li et al. 2011). The cumulative strain in samples not reaching failure in 1000 cycles remained below, or marginally exceeded, the static failure strain. Strain-controlled tests cycled from zero strain to the static failure strain (Åhnberg and Larsson 2012) initially mobilised deviator stress exceeding static strength. Cyclic stress in these tests then reduced to a stable value, below the stress causing failure in similar numbers of cycles in stress-controlled tests. Correspondence of this stable stress to the threshold stress was not investigated; estimating threshold stress from strain-controlled tests would require fewer tests than stress-controlled methods and could facilitate more comprehensive studies into factors affecting threshold stress.

8.0 Conclusions

This paper demonstrates the following factors for heavy haul roads produce a fundamentally different situation from conventional pavements:

- **Magnitude of load.** As a result of the large stressed zone from interaction of wheel loads, the response of the subgrade and changes induced by loading are of greater importance whilst the load-spreading properties of the pavement (thin relative to the whole-vehicle stress bulb) are less important. Loads are closer to bearing capacity due to the temporary nature of the roads and local yield is more prevalent in deeper normally consolidated deposits, meaning plastic strains are significantly increased and the changes these induce need to be accounted for. Stress rotation may be as important as magnitude in describing failure risk.
- **Increased load duration.** Slower loading rates, particularly for the high intensity loads and large strains expected, result in greater subgrade damage and may result in reduced threshold stress compared to faster loading rates.
- **Lower repetition frequency.** Consolidation and strengthening occurs between applications, potentially increasing the threshold stress.
- **Design requirements**. Settlement is of lesser concern, since avoiding subgrade failure is of greater importance. The short design life means focus is likely to be on minimising cost rather than providing

robustness. Cyclic failure is postulated to be a kinematically unstable, divergent process, with strain and subgrade damage occurring rapidly once it is reached: measures must be in place to avoid initiating such a mechanism.

Given this extreme situation, the authors suggest design is supplemented with an observational approach. Pore water pressure monitoring is proposed to be the most useful indicator of failure risk, although it is of limited use in soils at risk of metastable liquefaction which can incur loss of strength at small strains and with small induced pore water pressures. These areas must be indentified and remediated before operations begin.

A number of kinematically unstable failure modes are well defined in the literature; shear banding on the Hvorslev Surface, tensile liquefaction and metastable liquefaction. Reaching these failure modes is fundamentally determined by accumulation of excess pore water pressure which, on a micro-scale, can be linked to loss of restraint of 'strong' contact force networks. 'Strong' networks in granular materials 'buckle' once restraint is no longer sufficient; the micromechanical failure mechanism in clays is less well understood, however observed failure modes and DEM simulated behaviour of normally consolidated clays suggests the mechanism to be similar. Factors influencing the threshold stress which governs these cyclic failures are not fully understood and further research into this area is recommended.

Wet-of-critical metastable liquefaction is caused by breakages in the contact network and loss of particle equilibrium. There is good agreement in the literature that this phenomenon is heavily dependent upon soil fabric, which can develop anisotropy from stress history. Uniformly graded coarse soils, often of concern in earthquake engineering literature, may not be liquefied by slower heavy haul traffic if drainage during load occurs. However composite soils, which in some cases carry greater liquefaction risk, have lower permeability. Liquefaction risk levels associated with slow loading rates are not as well understood and this interaction between liquefaction risk, permeability and threshold stress merits further study.

Care must be taken in densifying liquefiable subgrades as induced anisotropy can reduce, rather than increase, liquefaction resistance. In particular, principal stress rotation under transient loads must be considered. Further research into modelling distribution of transient stress, principal axes rotation and the relative development of degradation in compression and extension zones is recommended.

Treating excess pore pressure from cyclic load as induced overconsolidation has been successful in a number of studies. Changes in strength and resilient modulus following large strains relate strongly to the stress state and induced pore water pressure. At smaller strain levels this is less apparent; the authors suggest this to be due to fabric rearrangement.

Drainage between loads is found to strengthen normally consolidated soil, implying increased threshold stress. This effect is currently not well understood and merits further research. Apparent overconsolidation is reduced by drainage, unless large volume change occurs, as in soils prone to wet-of-critical metastable liquefaction. This implies significant restructuring. Settlement may be of concern in such circumstances.
In clay soils, particularly, there is good agreement that strength and pore water pressure accumulation is load application rate dependent. Threshold stress relationships developed at faster rates may not apply to slow heavy haul road situations. Exploring links between rheology and rate dependent deformation and degradation is recommended as this may lead to more unified relationships, allowing more information on cyclic response and factors influencing threshold stress to be derived from a smaller number of carefully selected test conditions.

Acknowledgements

The authors acknowledge the financial support for this research provided by the University of Birmingham and the Engineering and Physical Sciences Research Council (EPSRC).

References

Åhnberg, H., and Larsson, R. 2012. Strength degradation of clay due to cyclic loadings and enforced deformation. Swedish Geotechnical Institute Report No. 75, Swedish Geotechnical Institute, Linkoping.

Allman, M. A., and Atkinson, J. H. 1992. Mechanical properties of reconstituted Bothkennar soil. Geotechnique 42(2): 289-301.

Anandarajah, A. 2000. On influence of fabric anisotropy on the stress/strain behavior of clays. Computers and Geotechnics 27: 1-17.

Andersen, K. H., Kleven, A., and Heien, D. 1988. Cyclic Soil Data for Design of Gravity Structures. ASCE Journal of Geotechnical Engineering, 114(5): 517–539.

Andersen, K. H. 2009. Bearing capacity under cyclic loading - offshore, along the coast and on land. The 21st Bjerrum Lecture presented in Oslo, 23 November 2007. Canadian Geotechnical Journal, 46(5): 513-535.

Arthur, J. R., Rodriguez, J. I., Dunstan, T., and Chua, K. S. 1980. Principal Stress Rotation: A Missing Parameter. ASCE Journal of the Geotechnical Engineering Division 106(4): 419-433.

Atkinson, J. H. 2007. The mechanics of soils and foundations (2nd Ed). Taylor and Francis.

Been K., and Jefferies, M.G. 1985. A state parameter for sand. Geotechnique 35(2): 99-122.

BSI (British Standards Institution). 1986. BS 8004:1986 Code of practice for foundations.

Brown, S. F., Lashine, A. K. F., and Hyde, A. F. L. 1975. Repeated load triaxial testing of a silty clay. Geotechnique 25(1): 95-114.

Brown, S. F., Andersen, K. H., and McElvaney, J. 1977. The Effect of Drainage on Cyclic Loading of Clay. In Proceedings of the 9th International Conference of Soil Mechanics and Foundation Engineering, Tokyo, July 11-15 July 1977, pp. 195-200.

Brown, S. F. 1996. Soil mechanics in pavement engineering. Geotechnique 46(3): 383-426.

Brown, S.F., and Chan, F. W. K. 1996. Reduced rutting in unbound granular pavement layers through improved grading design. Proceedings of the Institution of Civil Engineers – Transport 117, Feb, 40-49.

Carter J.P., Booker, J. R., and Wroth, C. P. 1982. A Critical State Soil Model for Cyclic Loading. In Soil Mechanics - Transient and Cyclic Loads, Edited by G. N. Pande & O. C. Zienkiewicz. John Wiley & Sons Ltd. pp 219-252.

Chandler, R. J., and Forster, A. 2001. Engineering in Mercia Mudstone. CIRIA report C570, Construction Industry Research and Information Association, London.

D'Appolina, D. J., Poulos H. G., and Ladd C. C. 1971. Initial Settlement of Structures on Clay. ASCE Journal of the Soil Mechanics and Foundations Division 97(10): 1359-1377.

Davis, E. H., and Poulos, H. G. 1972. Rate of settlement under two-and three dimensional conditions. Geotechnique 22(1): 95-114.

Dewhurst, D. N., Brown, K. M., Clennell, M. B., and Westbrook, G. K. 1996. A comparison of the fabric and permeability anisotropy of consolidated and sheared silty clay. Engineering Geology 42: 253-267.

Díaz-Rodriguez, J. A., and López-Molina, J. A. 2008. Strain thresholds in soil dynamics. 14th World Conference on Earthquake Engineering. October 12-17th 2008, Beijing, China. .

Doanh, T., Finge, Z., and Boucq, S. 2012. Effects of Previous Deviatoric Strain Histories on the Undrained Behaviour of Hostun RF Loose Sand. ASCE Journal of Geotechnical and Geological Engineering 30: 697-712.

Frost, M. W. 2000. The performance of pavement foundations during construction. Loughborough University.

Frost, M.W, Fleming, P.R, and Rogers, C. D. F. 2004. Cyclic triaxial tests on clay subgrades for analytical pavement design. ASCE Journal of Transportation Engineering 130(3): 378-386.

Gong G. 2008. DEM Simulations of Drained and Undrained Behaviour. Ph.D thesis, University of Birmingham Department of Civil Engineering, Birmingham, U.K.

Gräbe, P. J., and Clayton, C. R. I. 2009. Effects of Principal Stress Rotation on Permanent Deformation in Rail Track Foundations. ASCE Journal of Geotechnical and Geoenvironmental Engineering 135(4) pp.555-566.

Gratchev, I. B., Sassa, K., Osipov, V. I., and Sokolov, V. N. 2006. The liquefaction of clayey soils under cyclic loading. Engineering Geology 86: 70-84.

Gu, X., Huang, M., and Qian, J. 2013. DEM investigation on the evolution of microstructure in granular soils under shearing. Granular Matter 16, 91-106.

Guan, G. S., Rahardjo, H., Choon, L. E. 2010. Shear Strength Equations for Unsaturated Soil under Drying and Wetting. ASCE Journal of Geotechnical and Geoenvironmental Engineering 136: 594-606.

Heath, D. L., Shenton, M. J., Sparrow, R. W., and Waters, J. M. 1972. Design of Conventional Rail Track Foundations. ICE Proceedings 51(2): 251-267.

Hyde, A. F. L. 1974. Repeated load triaxial testing of soils. PhD thesis, University of Nottingham Department of Civil Engineering, Nottingham. U.K.

Ishihara, K., and Towhata, I. 1982. Dynamic Response Analysis of Level Ground based on the Effective Stress Method In Soil Mechanics - Transient and Cyclic Loads, Edited by G. N. Pande & O. C. Zienkiewicz. John Wiley & Sons Ltd. pp 133-172.

Jaquin, P. A., Augarde, C. E., Gallipoli, D., and Toll, D. G. 2009. The strength of unstabilised rammed earth materials. Geotechnique 59(5): 487-490.

Keedwell, M. J. 1984. Rheology and Soil Mechanics. Taylor and Francis

Kruyt, N.P., and Rothenburg, L. 2006. Shear strength, dilatancy, energy and dissipation in quasi-static deformation of granular materials. Journal of Statistical Mechanics: Theory and Experiment. doi:10.1088/1742-5468/2006/07/P07021.

Kruyt, N. P. 2010, Micromechanical study of plasticity of granular materials; Comptes Rendus Mecanique 338: 596-603.

Lade, P. V. 1994. Instability and Liquefaction of Granular Materials. Computers and Geotechnics 16: 123-151.

Li, L., Dan, H., Wang, L. 2011. Undrained behavior of natural marine clay under cyclic loading. Ocean Engineering 38: 1792-1805.

Little, P. H. 1992. The design of unsurfaced roads using geosynthetics. University of Nottingham Department of Civil Engineering.

Mammoet Europe B.V, 2015a. Industrial Transport Solutions [online]. Available from www.mammoet.com/en/Equipment/Transport [cited 18 February 2015].

Mammoet Europe B.V, 2015b. Case Studies [online]. Available from www.mammoet.com/en/Projects [cited 18 February 2015].

Marto, A. 1998. Pore Pressure Response of Undrained Two-Way Loading of Silt. Jurnal kejuruteraan (Journal of Engineering) 11(1): 35-63, Malaysia.

Muhunthan, B.,and Worthen, D. L. 2011. Critical state framework for liquefaction of fine grained soils. Engineering Geology 117: 2-11.

Ng, C. W. W., and Zhou, C. 2014. Cyclic behaviour of an unsaturated silt at various suctions and temperatures; Geotechnique 64(9): 709-720.

Nicot, F., and Darve, F. 2010. Multiscale analysis of failure. In Micromechanics of Failure in Granular Geomaterials, Edited by F. Nicot & R. Wan., ISTE and John Wiley & Sons. pp. 1-34.

Nouguier-Lehon, C. 2010. Effect of the grain elongation on the behaviour of granular materials in biaxial compression; Comptes Rendus Mecanique 338: 587-595.

Nova, R. 2010. Controllability of Geotechnical Tests and their Relationship to the Instability of Soils. In Micromechanics of Failure in Granular Geomaterials, Edited by F. Nicot & R. Wan., ISTE and John Wiley & Sons. pp. 1-34.

O'Reilly, M.P., Brown, S.F., and Austin, G. 1988. Some Observations on the Creep Behaviour of a Silty Clay. In Proceedings of the International Conference on Rheology and Soil Mechanics Edited by M. J. Keedwell, Coventry, 12-16 Sept 1988, Elsevier Applied Science. pp. 44-58.

O'Riordan, N. J. 1991. Effects of cyclic loading on the long term settlement of structures. In Cyclic Loading of Soils: from theory to design Edited by M. P. O'Reilly, S. F. Brown, Blackie and Son Ltd, Glasgow and London pp 411-430.

Osman, A. S., and Boulton, M. D. 2005. Simple plasticity-based prediction of the undrained settlement of shallow circular foundations on clay. Geotechnique 55(6), 435-447.

Overy, R. F. 1982. The Behaviour of Anisotropically Consolidated Silty Clay Under Cyclic Loading. Ph.D Thesis, University of Nottingham Department of Civil Engineering, Nottingham, U.K.

Pender, M. J. 1982. A model for the cyclic loading of overconsolidated soil. In Soil Mechanics - Transient and Cyclic Loads, Edited by. G. N. Pande & O. C. Zienkiewicz, John Wiley & Sons Ltd.pp 283-311.

Pérez, I., and Gallego, J. 2010. Rutting prediction of a granular material for base layers of low-traffic roads. Construction and Building Materials 24: 340-345.

Ravi, K., Dash, S., Vogt, S., and Braeu, G. 2014. Behaviour of Geosynthetic Reinforced Unpaved Roads Under Cyclic Loading. Indian Geotechnical Journal 44(1): 77-85.

Sazzad, M., and Suzuki, K. 2010. Micromechanical behavior of granular materials with inherent anisotropy under cyclic loading using 2D DEM. Granular Matter 12: 597-605.

Schofield, A., and Wroth, P. 1968. Critical State Soil Mechanics. McGraw Hill, London.

Selig, E. T., and Chang, C. S. 1981. Soil failure modes in undrained cyclic loading. ASCE Journal of Geotechnical Engineering Division 107 (5): 539-551.

Sharp, R.W.,and Booker, J. R. (1984). Shakedown of pavements under moving surface loads. ASCE Journal of Transportation Engineering 110(1), 1-14.

Singh, A., and Mitchell, J. K. 1968. General Stress-Strain-Time Function for Soils. ASCE Journal of the Soil Mechanics and Foundations Division 94(1): 21-46.

Sivathayalan, S.,and Vaid, Y.P. 2002. Influence of generalized initial state and principal stress rotation on the undrained response of sands. Canadian Geotechnical Journal 39:63-76.

Skempton, A.W. 1995. Embankments and Cuttings on the early Railways. Construction History 11: 33-49, The Construction History Society.

Soroush, A., and Ferdowsi, B. 2011. Three dimensional discrete element modeling of granular media under cyclic constant volume loading: A micromechanical perspective; Powder Technology 212: 1-16.

Thornton, C. 2000. Numerical simulations of deviatoric shear deformation of granular media. Geotechnique 50(1): 43-53.

Togrol, E., and Güler, E. 1984. Effect of repeated loading on the strength of clay; Soil Dynamics and Earthquake Engineering 3(4): 184-190.

Toll, D. G. 1990; A framework for unsaturated soil behaviour; Geotechnique 40(1): 31-44.

Toll, D.G. and Ong, B. H. 2003. Critical-state parameters for an unsaturated residual sandy clay; Geotechnique 53(1): 93-103.

Vaid, Y. P. 1988. Time Dependent Shear Deformation of Clay. In Proceedings of the International Conference on Rheology and Soil Mechanics Edited by M. J. Keedwell, Coventry, 12-16 Sept 1988, Elsevier Applied Science. pp. 123-129.

Wang, S., Luna, R., and Onyejekwe, S. 2015. Postliquefaction behavior of low-plasticity silt at various degrees of reconsolidation. Soil Dynamics and Earthquake Engineering 75, 259-264.

Ward, S. J. 1983. The stability of a silty clay under repeated loading. Ph.D thesis, Loughborough University, Loughborough, U.K.

Wei, L. M., and Yang, J. 2014. On the role of grain shape in static liquefaction of sand–fines mixtures. Geotechnique 64(9): 740-745.

Werkmeister, S., Dawson, A. R., and Wellner, F. 2004. Pavement Design Model for Unbound Granular Materials. ASCE Journal of Transportation Engineering 130(5): 665-674.

Wolff, H., and Visser, A. T. 1994. Incorporating elasto-plasticity in granular pavement design. Proceedings of the Institution of Civil Engineers – Transport 105, Nov.: 259-272.

Xiao, J., Juang, C. H., Wei, K., and Xu, S. 2014. Effects of Principal Stress Rotation on the Cumulative Deformation of Normally Consolidated Soft Clay under Subway Traffic Loading. ASCE Journal of Geotechnical and Geoenvironmental Engineering 140(4): 04013046.

Xu, X. M., Ling, D. S., Ghen, Y. P., and Chen, Y. M. 2015. Correlation between liquefaction resistance and shear wave velocity of granular soils: a micromechanical perspective. Geotechnique 65(5), 337-348.

Yamamuro, J. A., and Lade, P. V. 1999. Experiments and modelling of silty sands susceptible to static liquefaction. Mechanics of Cohesive-Frictional Materials 4: 545-564.

Zdravković, L., and Jardine, R. J. 2001. The effect on anisotropy of rotating the principal stress axes during consolidation. Geotechnique 51(1): 69-83.

Zhao, X., and Evans, T. M. 2011. Numerical analysis of critical state behaviors of granular soils under different loading conditions. Granular Matter 13: 751-764

Zhao, J., Sloan, S. W., Lyamin, A. V., and Krabbenhøft, K. 2008. Bounds for shakedown of cohesive-frictional materials under moving surface loads. International Journal of Solids and Structures 45, 3290-3312.

List of Tables

Table 1: Soil properties used in elastic analysis of stress under multi-wheeled heavy haul vehicle

Layer	**Model**	**Reference pressure, p'_{ref} (kPa)**	**Elastic modulus at reference pressure, K (kPa)**	**Exponent, n (-)**	**Poisson's ratio (-)**	**Unit weight (kPa)**
Unbound pavement	Nonlinear elastic $E = K\,(p'/p'_{ref})^n$	100	50,000	0.5	0.26	21
Subgrade	Linear elastic	**Elastic Modulus, E (kPa)**		**Poisson's Ratio(-)**		**Unit weight (kPa)**
		13225		0.499		17

List of Figures

Figure 1: Heavy equipment being transported on a platform composed of Self-Propelled Modular Transporters (SPMTs), Courtesy of and ® of Mammoet (2015b).

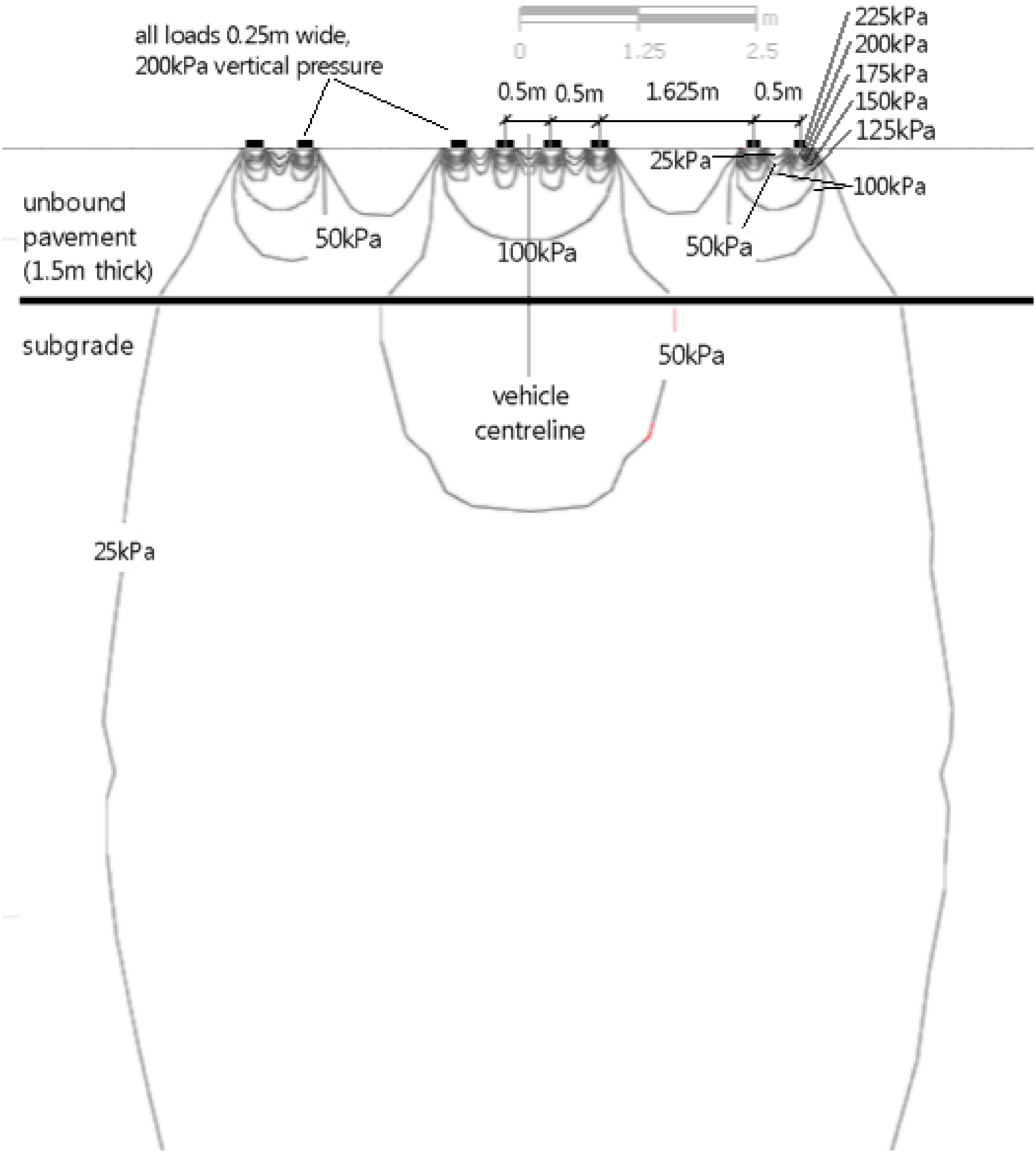

Figure 2: Contour plot showing increase in vertical total stress from elastic plane-strain analysis of a 6m wide platform composed of multiple SPMTs, assuming a non-linear elastic unbound pavement and linear elastic clay subgrade based on parameters from Table 1. Each wheel load is a 0.25m wide strip applying 200kPa vertically to the road surface.

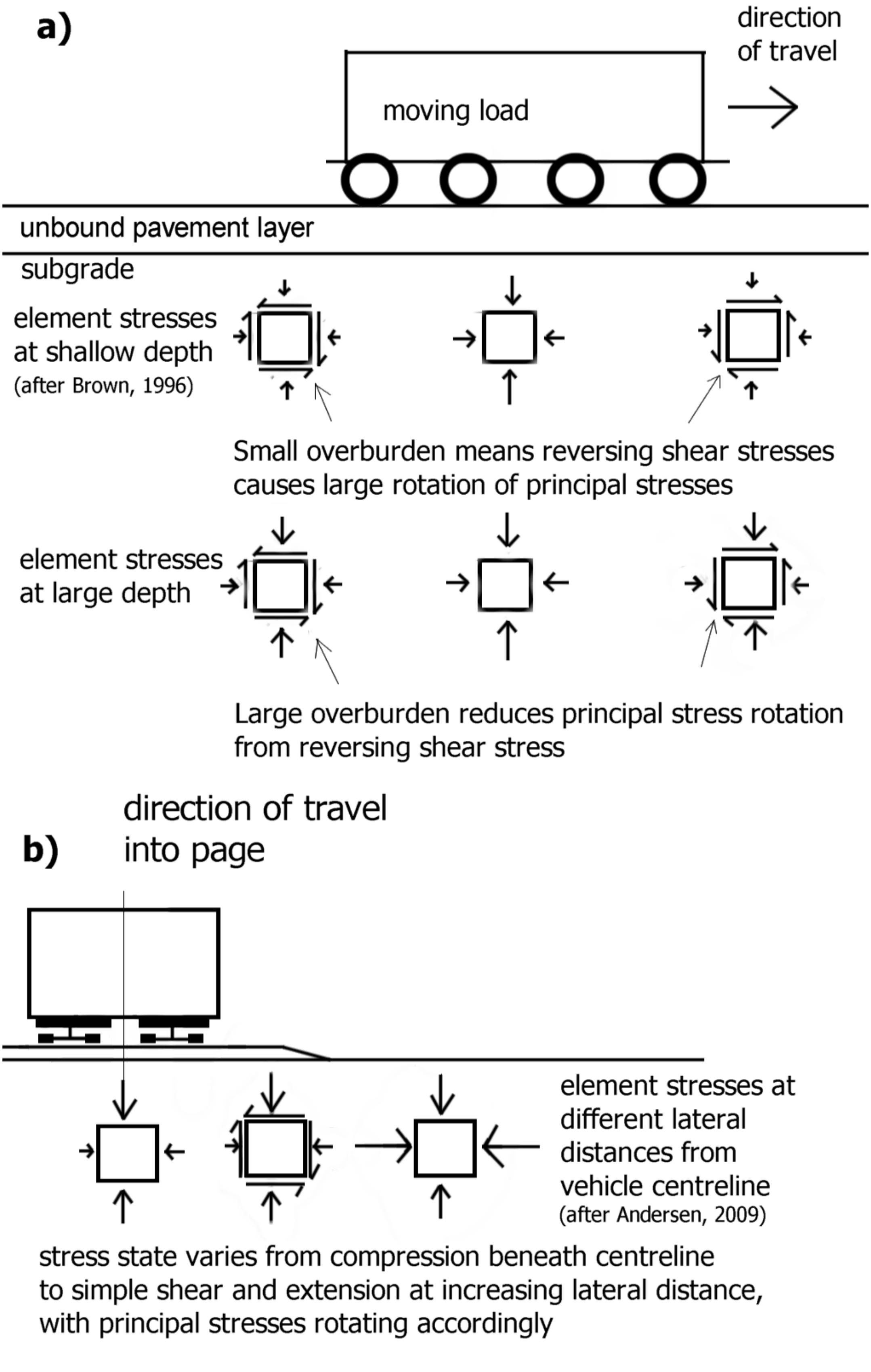

Figure 3: Rotation of principal stresses in longitudinal and transverse directions resulting from passage of a heavy haul vehicle

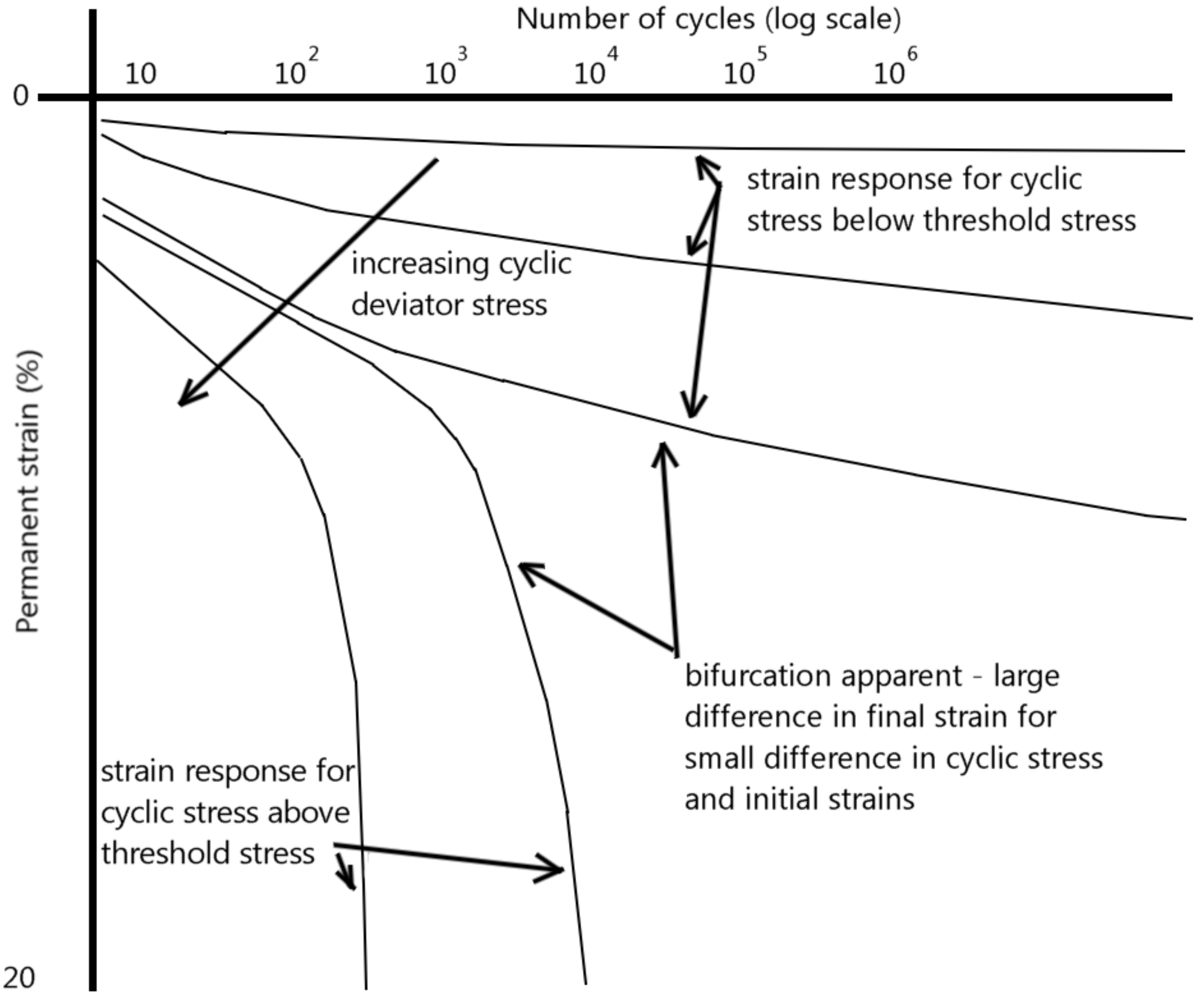

Figure 4: Illustration of cyclic failure as a bifurcation dependent upon stress intensity, after Heath et al. (1972)

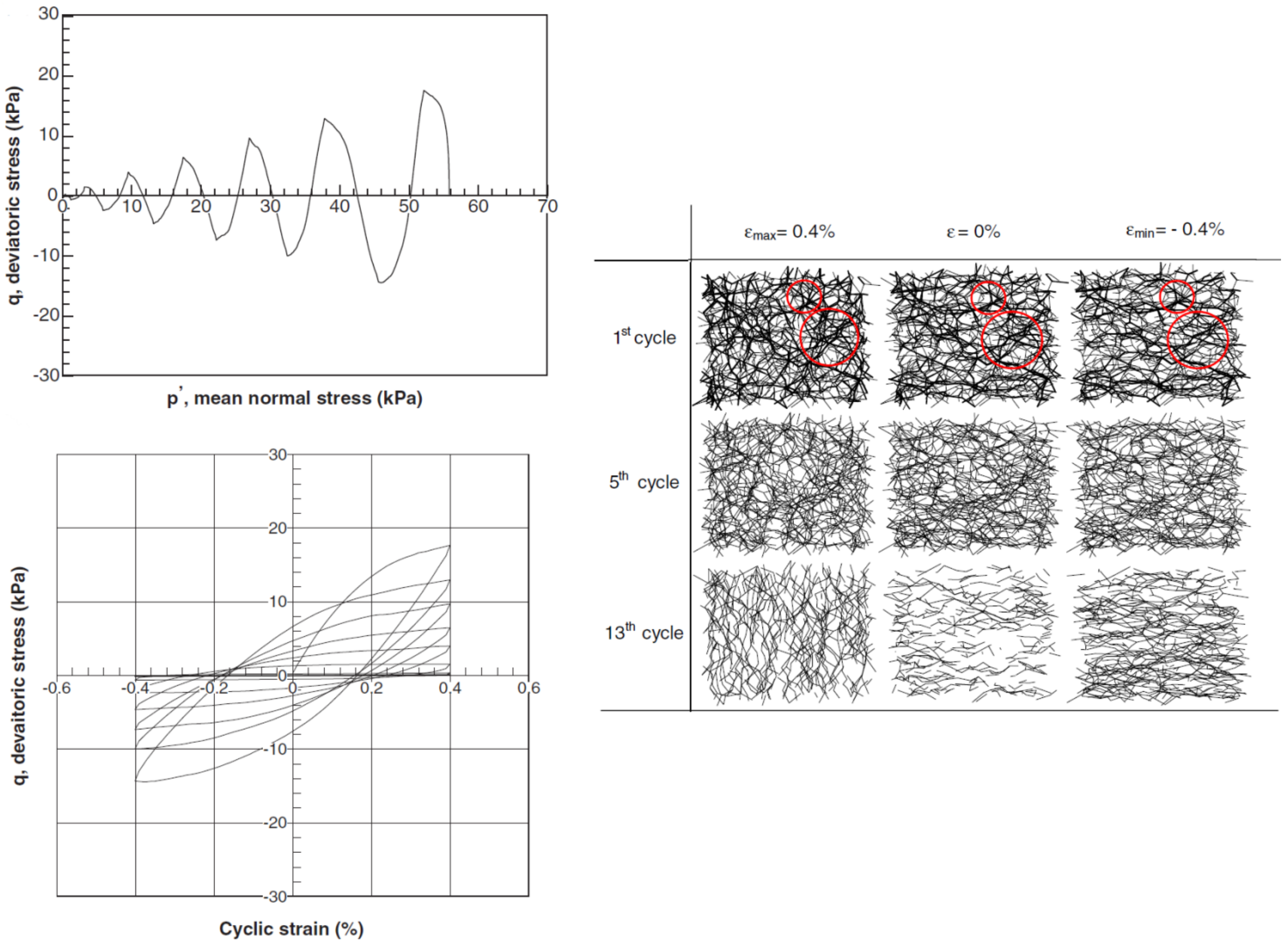

Figure 5: Stress-strain response of DEM simulation of undrained cyclic load (left) and vector representations of strong contact force (i.e. greater than average inter-particle force) network (right) displaying reduction in strong inter-particle force magnitude, increasing anisotropy and eventual liquefaction with regions of disconnected strong contacts, taken from Soroush and Ferdowsi (2011)

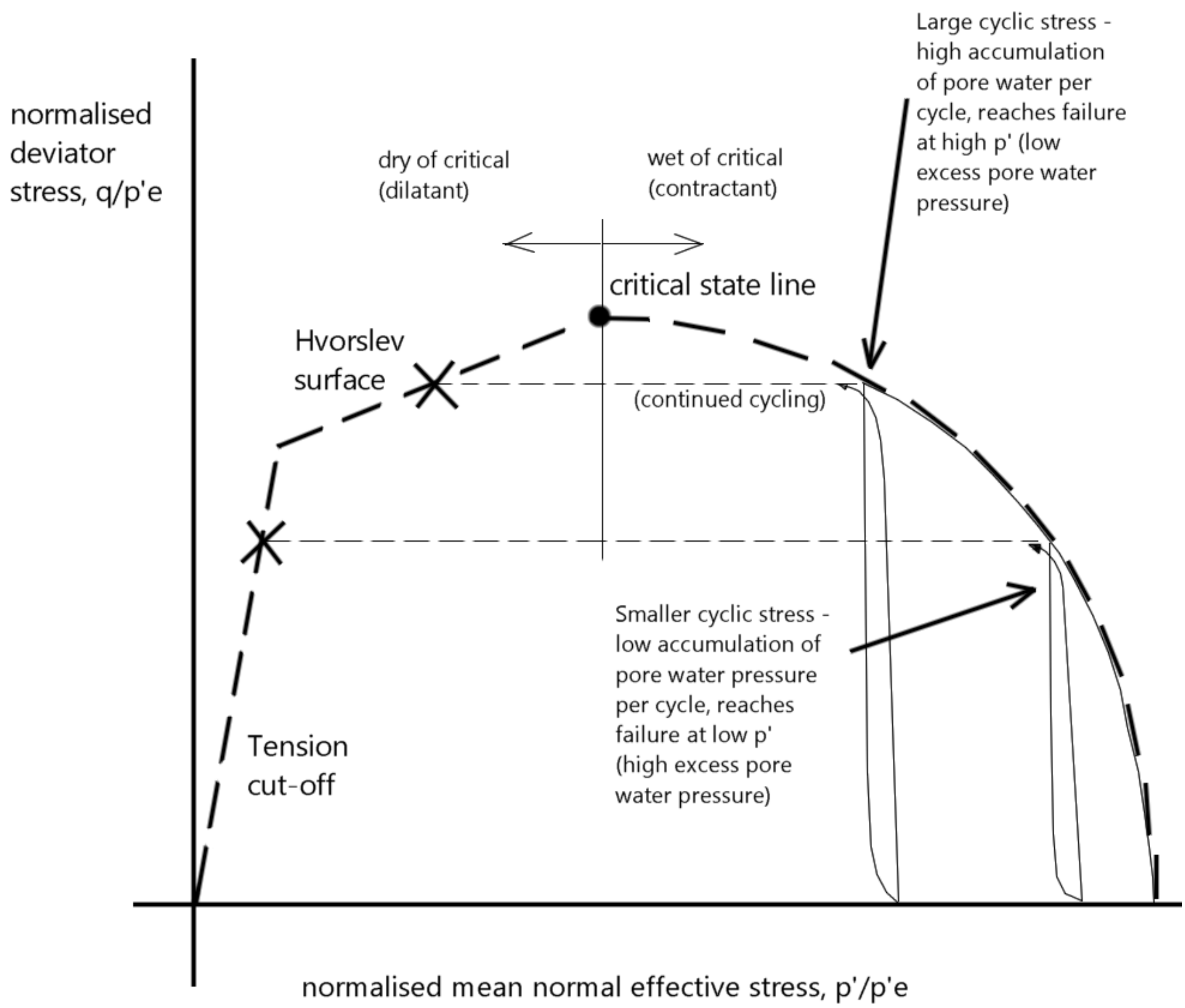

Figure 6: Representation of undrained cyclic stress paths in normalised stress invariant space for normally consolidated soil, assuming failure on the Hvorslev Surface or tension cut-off.

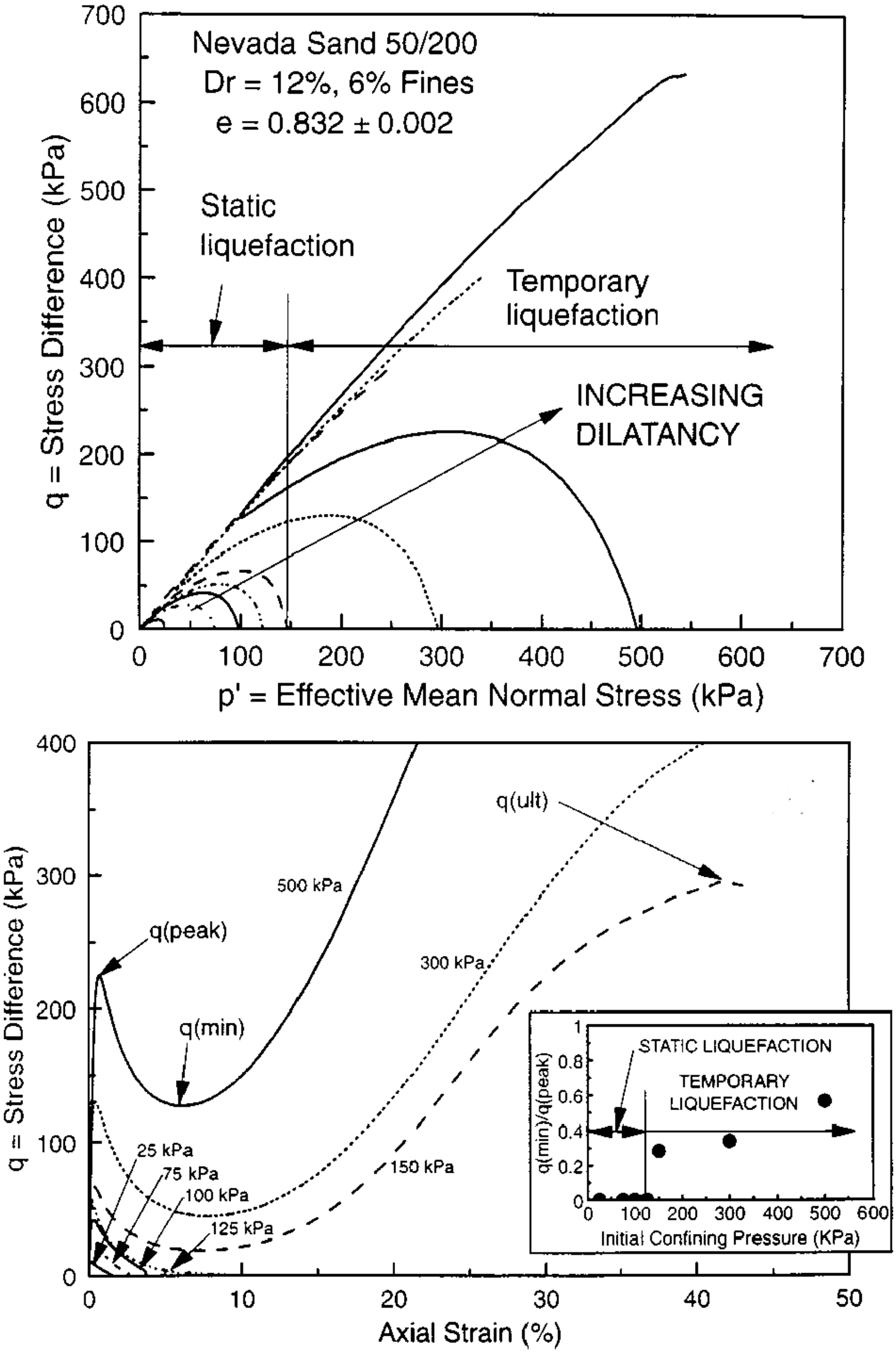

Figure 7: Effective stress paths (upper) and stress-strain relationships (lower) for Undrained static triaxial compression tests on loose silty sand, showing static liquefaction (strain softening following the q(peak) label) at small strain and subsequent recovery (labelled as q(ult)), at large strains (taken from Yamamuro & Lade, 1999). Pressures next to lines on the lower stress-strain plot indicate confining pressure at the start of each test.

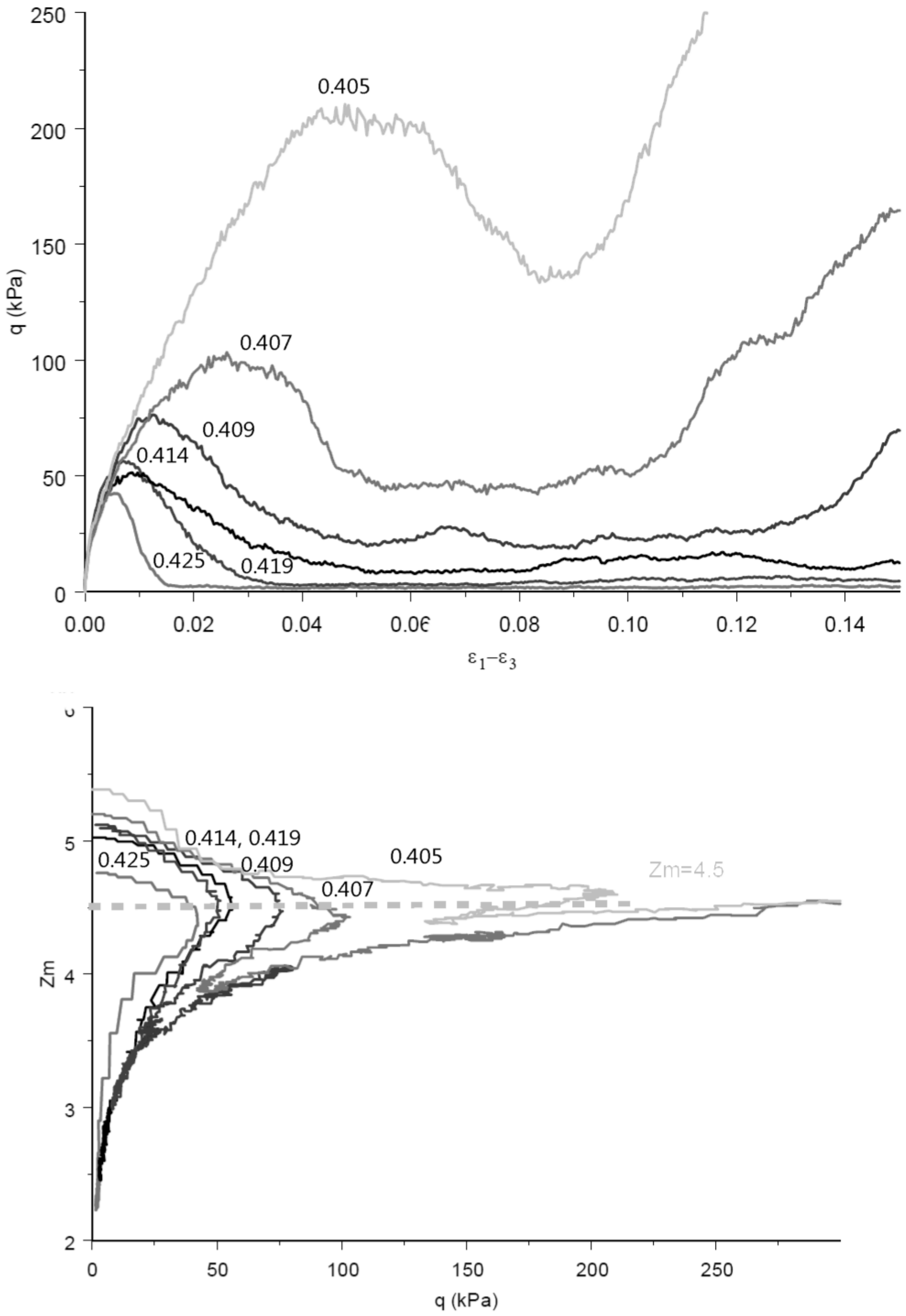

Figure 8: Comparison of static liquefaction in a DEM assembly to evolution of mechanical coordination number (Z_m) and formation of a mechanism with loss of particle static equilibrium, taken from Gong (2008). Above – deviator stress as a function of strain for various assembly porosities, below - mechanical coordination number as a function

of deviator stress, illustrating peak deviator stress coinciding with the critical coordination number of 4.5. Numbers above curves indicate assembly porosity.

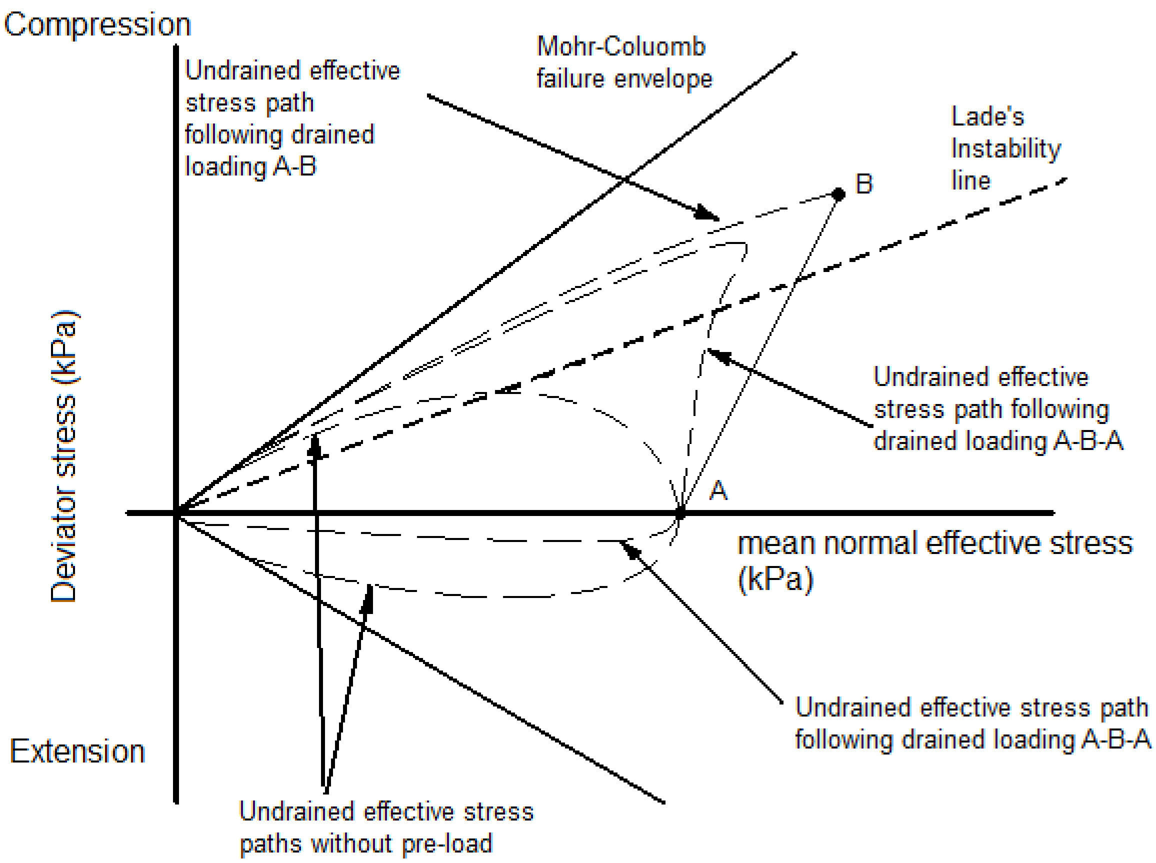

Figure 9: Undrained triaxial tests in undrained loose sand demonstrating static liquefaction from a small undrained increment above the instability line and load-induced anisotropy, displaying increasing compression resistance and reduced extension resistance after a cycle of drained load, after Doanh et al. (2012).

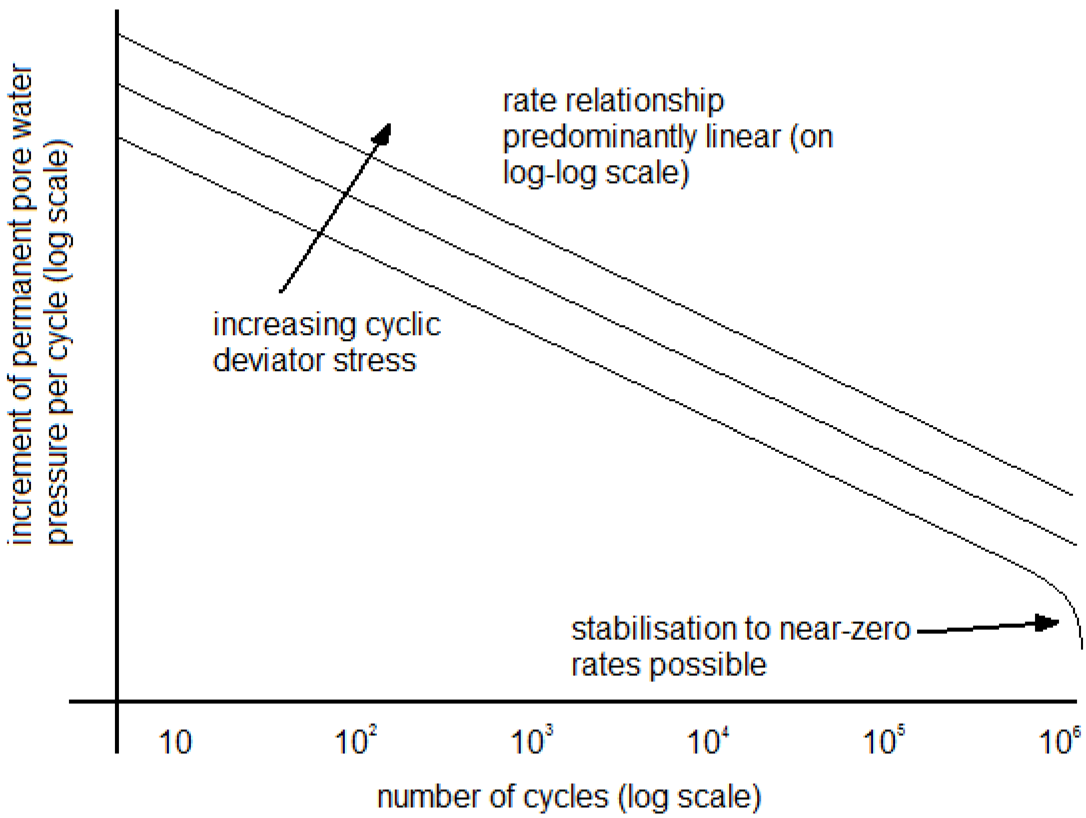

Figure 10: Development of pore water pressures under cyclic loading, applicable to one-way cyclic loading (after Hyde, 1974 and Ward, 1983) and two-way cyclic loading (after Marto, 1998); this relationship also applies to accumulation of permanent strains under one-way cyclic loading (after Hyde, 1974 and Ward, 1983).

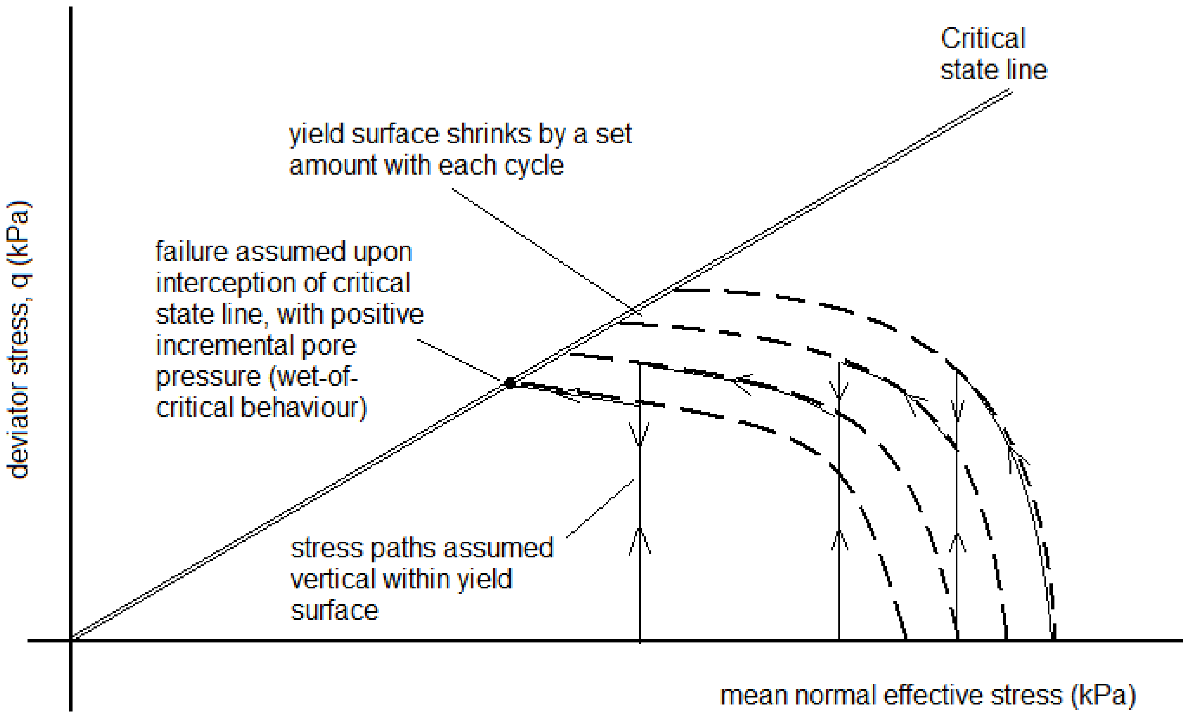

Figure 11: Cyclic loading modelled as shrinkage of wet-of-critical yield surface, after Carter et al (1982). Note the stress state is implied to reach failure from the wet-of-critical yield surface.

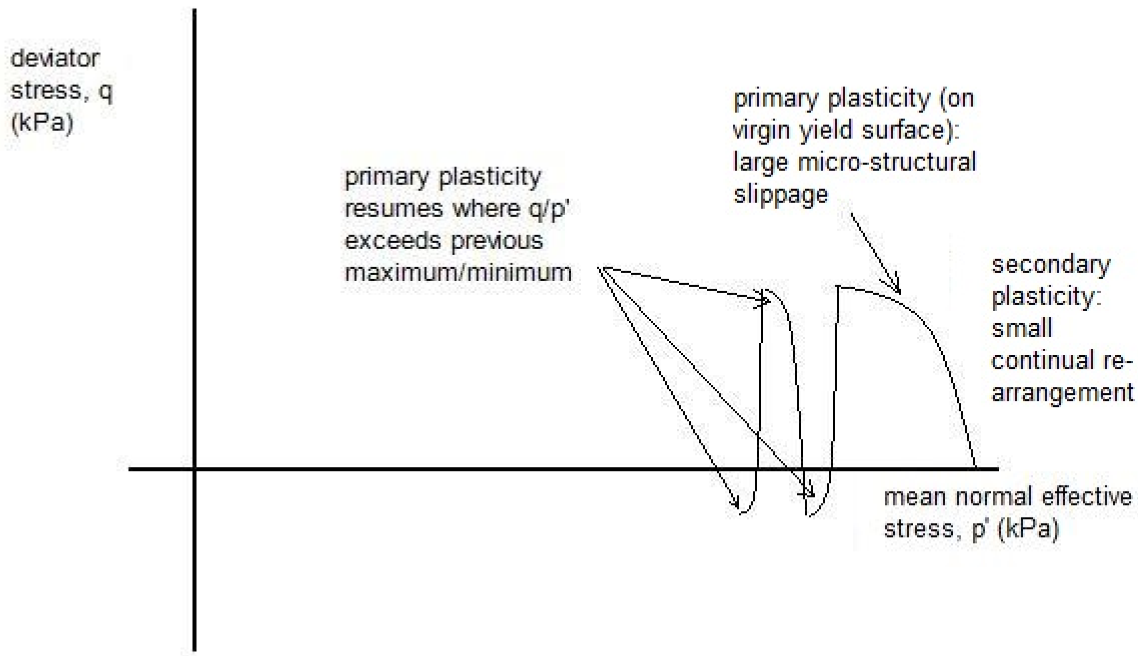

Figure 12: Definition of primary and secondary plasticity, after Isihara and Towhata (1982).

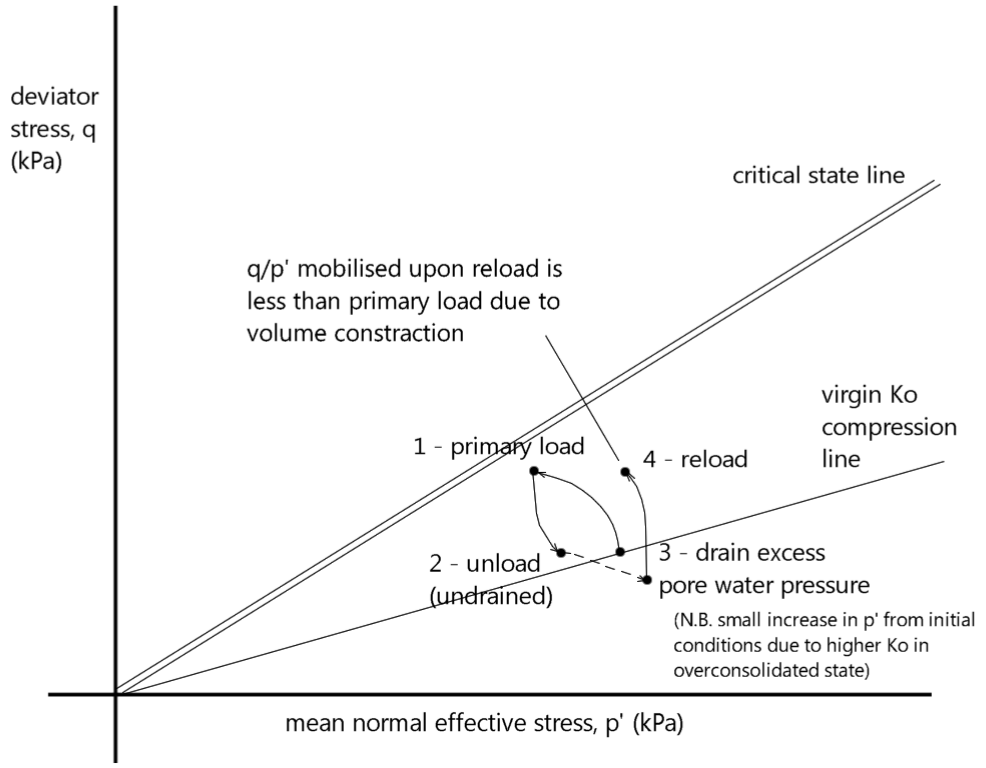

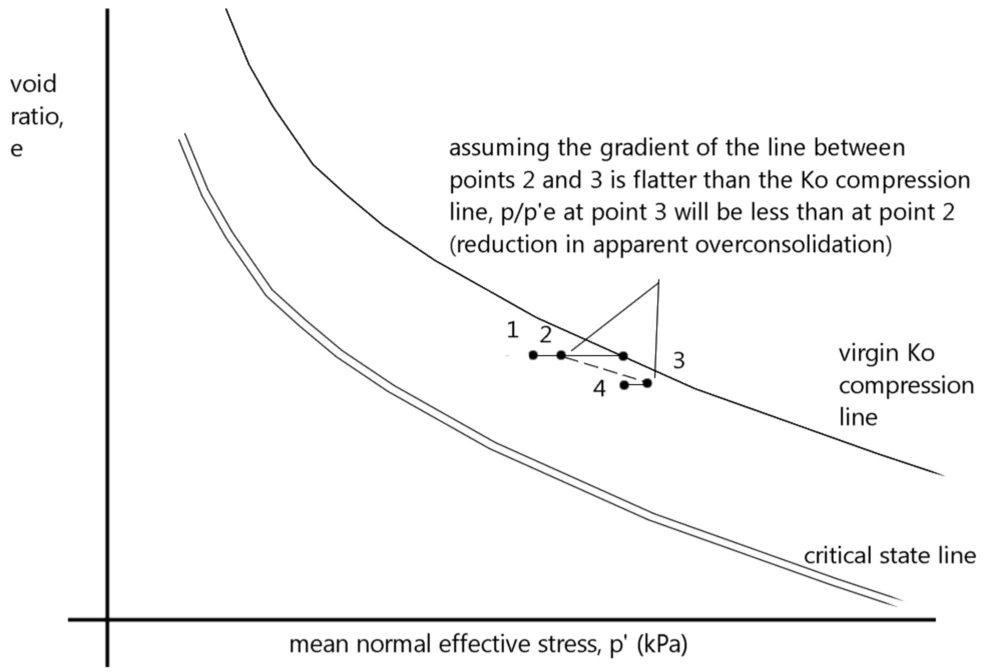

Figure 13: Development of hysteretic cyclic stress-strain loops (a, b and c) and normal contact force anisotropy (d, e and f) as a function of strain under cyclic load, taken from Sazzad & Suzuki, 2010. d) is for all contacts, e) is for strong contacts only and f) is for weak contacts only. N.b. δ refers to the angle of orientation of the long axis on an oval particle with the horizontal axis.

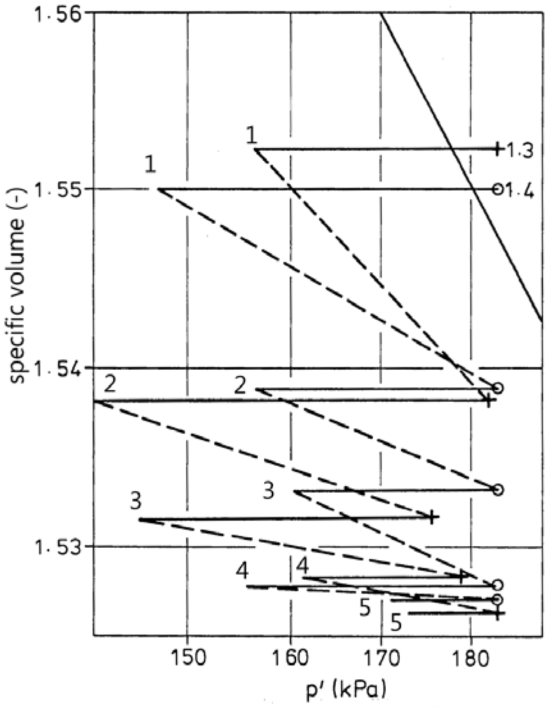

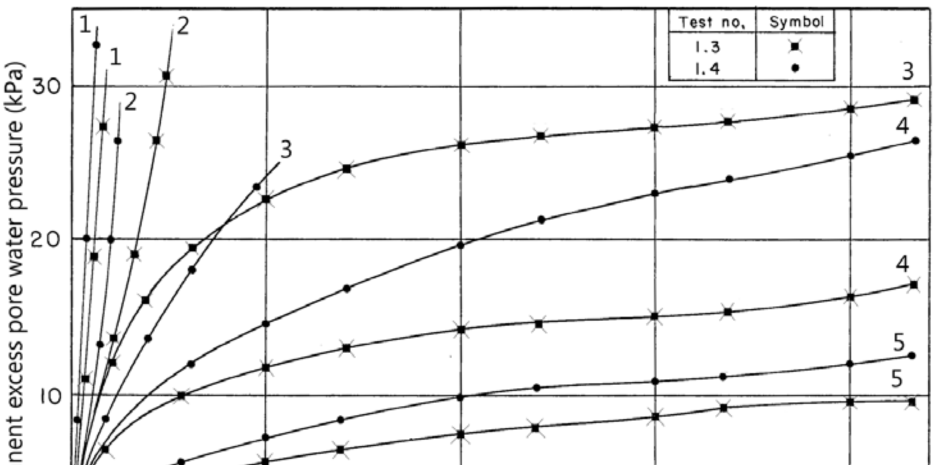

Figure 14: Increase in cyclic resistance as a result of drainage intervals (above) following each sequence, modified from Overy (1982), illustrating a bifurcation and implying increasing threshold stress. Numbers adjacent to curves refer to the day in sequence of testing, with drainage intervals provided between each. Changes to specific volume during drainage periods (below) modified from Overy (1982), showing initially steep volume change gradient becoming shallower.

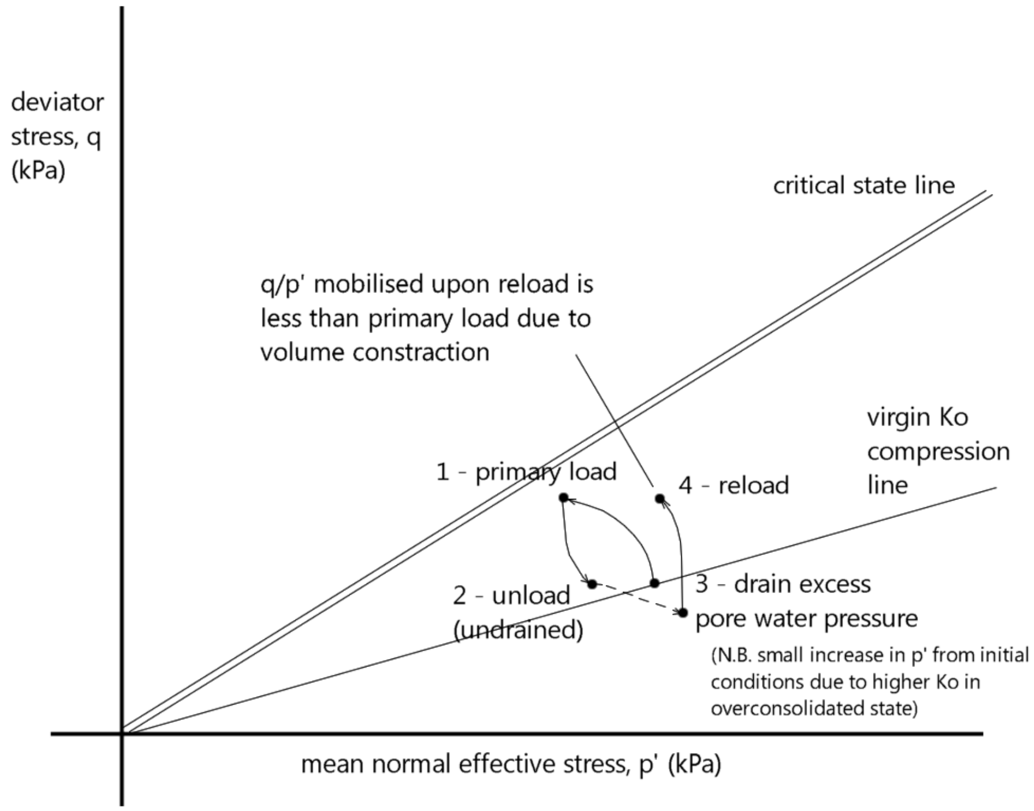

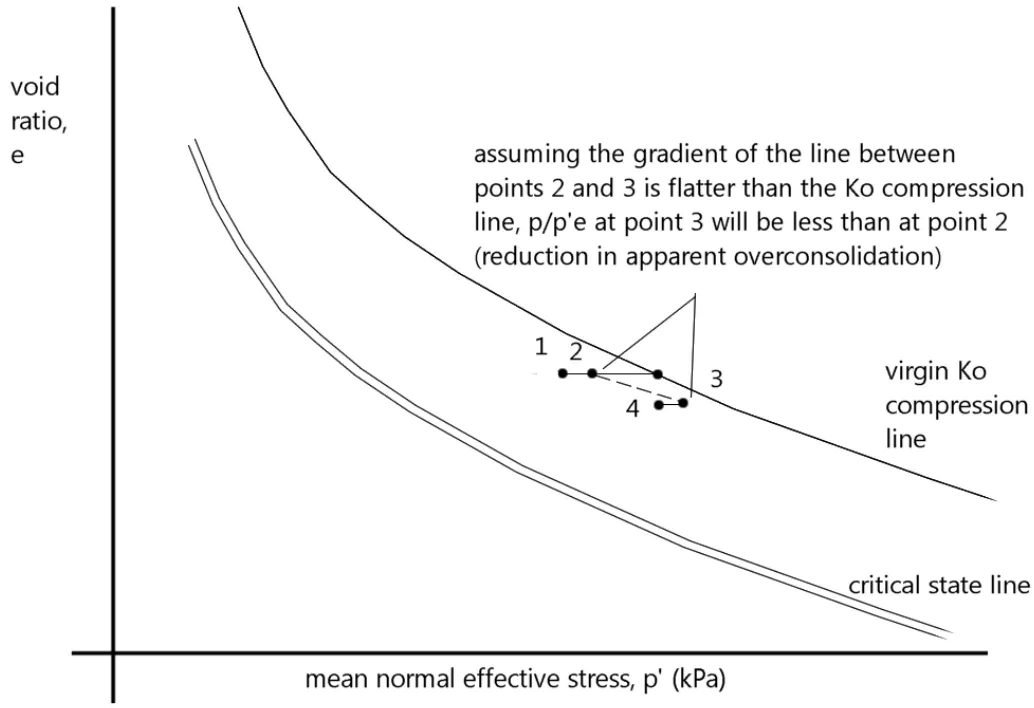

Figure 15: Representation of cyclic stress paths with full drainage of excess pore water pressure between loads in e, q, p' space